
UNIVERSITY OF PADOVA

Department of Land, Environment, Agriculture and Forestry

Second Cycle Degree (MSc)
in Forest Science

# The effects of drought in wood anatomical traits of Austrian pine (*Pinus nigra*) in Venosta valley

*Supervisor*
*Prof.* Marco Carrer

*Co-supervisor*
*Dott*. Lucrezia Unterholzner

*Submitted by*
Claudia Citron

ACADEMIC YEAR 2021-2022

# CONTENTS

## ABSTRACT

In recent decades, drought events have increased in frequency and intensity all over the world, inducing more and more cases of forest decline. Forest mortality episodes are expected to increase in the near future, in parallel with the increasing frequency of drought events. All this represents a challenge for trees, which can withstand occasional and mild episodes of water stress, but could hardly survive in face of their substantial increase in frequency and intensity.

An example is *Pinus nigra*, a species that generally shows a high tolerance to harsh environmental conditions, but whose geographical distribution is expected to shrink in the future. Indeed, increasingly drier climate, could likely negatively influence its xylem anatomical features and the consequent physiology of the species. In this thesis I investigated the effects of drought in wood anatomical traits of Austrian pine (*P. nigra*) in Venosta valley (Italy). In particular, through a dendro-anatomical approach, I retrospectively identified the differences between *non-declining (ND)* and *declining (D)* trees in terms of radial growth (ring width), cell size (lumen area), cell wall dimension (cell wall thickness) and number of cells per ring (cell number), considering a time-span of 75 years. Data collection and analysis was carried out with *ROXAS*, *R* and *Excel* programs.

The series of anatomical traits for the *D-ND* trees were correlated with climatic variables (temperature, precipitation and the SPEI-3 drought index).

Despite the similar trend for both groups analysed (*D-ND*), the results obtained showed a greater climatic sensitivity on the *declining* trees, and the differentiation of certain anatomical traits only in some years such as 1996 and 2007. The sudden mortality of certain trees, therefore, may probably be due to some other factors such as one or more subsequent extreme events and/or a pest outbreak, rather than the persistent drought of the area. This thesis underlines the need to obtain an accurate understanding of the forest response to this type of events, leaving room for further future investigations on this issue.



**Keywords**: Drought, *Pinus nigra*, Venosta valley, quantitative-wood-anatomy, forest decline.

## RIASSUNTO

Negli ultimi decenni, gli eventi di siccità sono aumentati in frequenza e intensità ovunque nel mondo, provocando sempre più casi di declino e mortalità nei popolamenti forestali. Si prevede che gli episodi di mortalità delle foreste aumenteranno nel prossimo futuro, parallelamente alla crescente frequenza e intensità degli eventi siccitosi. Tutto questo rappresenta un problema per gli individui arborei che ben possono sopravvivere a rari episodi di stress idrico, ma che si ritrovano in seria difficoltà di fronte ad un loro aumento consistente. Ne è un esempio il *Pinus nigra,* una specie che generalmente dimostra un'alta tolleranza ad ambienti particolarmente difficili, ma la cui distribuzione geografica si prevede verrà ridotta in futuro proprio a causa di un clima sempre più siccitoso in grado verosimilmente di influenzarne i tratti anatomici e la conseguente fisiologia. In questa tesi quindi, abbiamo studiato gli effetti della siccità nei tratti anatomici dello xilema del pino nero (*P. nigra*) in Val Venosta (Italia). In particolare, attraverso un approccio dendro-anatomico, sono state identificate, in termini di crescita radiale (larghezza dell'anello), dimensione cellulare (area del lume), dimensioni della parete (spessore della parete cellulare) e numero di cellule prodotte (numero di cellule per anello), le differenze tra gli alberi *non in declino* (*ND*) e gli alberi in *declino* (*D*) su un arco temporale di 75 anni. La raccolta e analisi dei dati è stata realizzata con i programmi di *ROXAS*, *R* ed *Excel*. Si sono così prodotte le serie dei tratti anatomici per le piante *D-ND* e calcolate le correlazioni climatiche tra tali parametri xilematici e le variabili di temperatura, precipitazione e indice di siccità SPEI-3. Nonostante l'andamento simile per entrambi i gruppi analizzati (*D-ND*), dai risultati ottenuti è emersa una maggiore sensitività climatica da parte delle piante in *declino*, con la differenziazione di certi tratti anatomici solo in alcuni anni come il 1996 e il 2007. La mortalità repentina di alcuni individui, quindi, deve essere probabilmente imputata a qualche altro fattore come uno o più eventi estremi successivi e/o un agente di disturbo biotico, piuttosto che alla persistente siccità dell'area. Tale tesi sottolinea quanto sia necessario avere un'accurata comprensione della risposta forestale a questo tipo di eventi, lasciando spazio a ulteriori future indagini su questo tema.

# 1) INTRODUCTION

Increasing frequency and intensity of drought events are reported worldwide and have been suggested to arise mainly from ongoing climate warming (IPCC, 2021). As consequence, vegetation belts start to shift upward or at higher latitudes and forest decline phenomena are already evident in several biomes (Savi et al., 2019), since drought can negatively affect forest ecosystems by triggering tree mortality. Moreover, mortality induced by water limitation is most likely to further expand in the future: the frequency and intensity of drought events is predicted to increase, especially in the Mediterranean basin and other areas subjected to seasonal water shortage (IPCC, 2021).

This constant rise of atmospheric temperature leads to an increase of the atmospheric moisture demand and consequently to a further rise of heat and drought of land surface at the same time (Mukherjee et al., 2018). An additional factor is the anthropogenic activity (such as urbanization, change in land use/land cover and industrialization) that, in conjunction with a lack of precipitations for an extended period, may cause a streamflow shortage known as hydrological drought (Kim and Jehanzaib, 2020). Furthermore, drought in combination with other unfavourable abiotic or biotic factors (like poor site conditions or pest outbreaks), can limit the living functions of plants leading to mortality at stand level (Manion, 1991).

Global forest die-off in response to drought shows how fast some forest ecosystem services, like the carbon sequestration ability, can be partially lost due to rapid trees vigour loss (Anderegg et al., 2015). An important portion of carbon stock of the world forests is stored in the northern hemisphere, but their functions are at risk: the increasingly hot climate is changing plant phenology, especially at high latitudes, extending their growing season (Pan et al., 2011). If the growing season is longer, it would be straightforward to think that, plants should have more time and longer favourable conditions to sequester a greater amount of atmospheric carbon dioxide (Puchi et al., 2020). However, there are some studies that stated the opposite: analysing the relation between climate change and tree growth in the northern hemisphere at the end of 20$^{th}$ century it has been noticed that warmer temperatures were frequently associated with a decrease in the plant growth rates because of the

presence of major water stress (Barber et al., 2000; Girardin et al., 2014; Walker and Johnstone, 2014).
Trees can easily survive to rare extreme events, but an excess in drought periods frequency and duration can cause their mortality (Lebourgeois et al., 2010). Investigating how trees react to drought will help to forecast which forests will be the most vulnerable (Pellizzari et al., 2016).

In this context, a powerful tool to explore tree responses to drought events is dendro-anatomy. With this tool, it is possible to obtain information about the drought-induced forest mortality, managing to go far back over the years. This approach analyses historic series of tree-ring anatomical traits that represent a new source of valuable climatic information. During every growing season, trees create a new ring which mirrors the weather conditions of that season; the features of tree-ring anatomy, (such as ring width, rings and cells density, cell wall thickness, lumen area etc.) can be considered useful proxies to better understand environmental variability (von Arx & Carrer, 2014).

To better appreciate which strategy the tree can use in case of water stress, it is useful to understand what are the fundamental anatomical elements that allow the plant to react in the case of water shortage.
Almost each part of a tree is constituted by wood, that is a porous and fibrous tissue formed by different type of cells, with specific functions like nutrients and water transportation, nutrient storage and mechanical support. There are two types of wood: the hardwood from angiosperm trees and softwood from gymnosperm trees (Buscarini et al., 2019). Since this thesis will deal with *Pinus nigra,* the focus will be on the last type of wood. The key softwood cells are called tracheids: their role consists in carrying water from the roots to the leaves thanks to their longitudinally elongated structure. Tracheids are connected one to the other by pits, small holes that allow the water movement among the cells, and in the gymnosperm, they are the main structure elements of the xylem. The latter is a tissue responsible mainly for water and sap transport, but it is also fundamental for the tree mechanical support. Thus, water is pulled up under tension from the roots to the leaves through the

tracheids, in a constant path called *the soil-plant-atmosphere-continuum* (McElrone et al., 2013)

Then, there are other anatomic structures with transport and storage roles for nutrients, which are respectively called cambium rays and parenchymatic rays. The cells produced from the cambium outwards create another tissue: the phloem. It is responsible for the transportation of the sucrose (obtained during photosynthesis) from the upper parts to the roots of the woody plant (Buscarini et al., 2019).

Generally, in areas with seasonal climate, the majority of conifers produce one tree ring per year; such tree ring can be divided in earlywood, built during spring/early summer and latewood, created in late summer. The typical cells of earlywood have thin cell walls and large lumen, while the cells of latewood have smaller lumen area with thicker cell walls. The transition between these two parts of the tree ring is usually well recognizable (especially in conifer), since the latewood is distinctively darker (Blasing & Fritts, 1976) (**Figure 1**). Another conifer's wood characteristic is the presence of resin canals (**Figure 1**): they have the function of secreting resin which is a substance that is necessary to defend the trees from fungi and general infections (Speer, 2010).

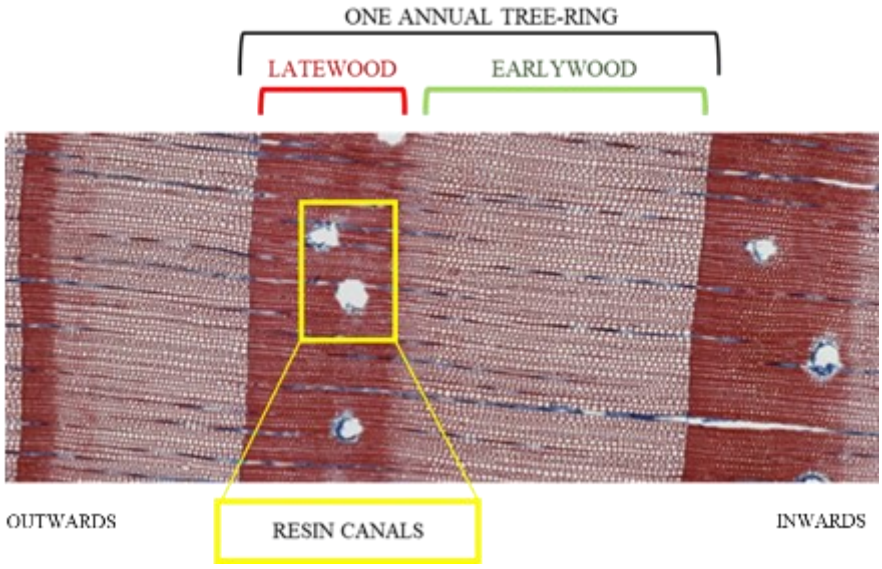


**Figure 1:** *Microscopic transversal section' slide of a Pinus nigra (personal elaboration).*

Since the general frame on plant anatomy has been addressed, it will be possible to better understand the physiological strategies adopted by trees in response to water stress.

As stated by Klemm, (2019)*: "patterns of climate-induced forest dieback are complex and physiological drivers of tree mortality still are insufficiently understood*". Despite gaps of knowledge still exist on the process behind tree mortality, there are a few main explanations that are broadly accepted (Martin-Benito et al., 2017):

- *the carbon-starvation hypothesis* which states that there's a carbon limitation at the source level due to stomatal closure and thus, a lower carbon assimilation (McDowell et al., 2008);
- *the reduction in meristematic activity and cambial enlargement* (Körner, 2003)*;*
- *the hydraulic failure* (Sala et al., 2010).

The decrease in soil water supply, together with the increase of evapotranspiration rate during drought periods, leads to cavitation of water columns in the xylem, causing a further reduction in the water supply (McDowell et al., 2008).

The plants' reaction to drought stress varies within a range between *isohydric strategy* (Jones, 1998) and *anisohydric strategy* (Martínez-Vilalta et al, 2014), due to the fact that stomatal and hydraulic response are closely co-regulated: in the first case, trees close stomata in order to reduce transpiration to keep xylem water potential within safety margins, but reducing the photosynthetic rates; instead, in the second strategy, trees maintain constant levels of stomatal conductance, but with the higher risk of embolism formation (Martin-Benito et al., 2017). Thus, when soil water availability decreases, water potential in xylem conduits decreases, reducing the safety margins against embolism formation. The capacity of the xylem to supply water becomes insufficient to sustain transpiration when critical water potential thresholds (specific for each species) are exceeded, and trees may also die due to drastic hydraulic failure (Savi et al., 2019; Tyree & Ewers, 1991; Nardini et al., 2013). Survival and health status of plants in water limited conditions mostly depend

on the individuals' hydraulic performance (i.e., vulnerability to drought induced embolisms), that in turn is strictly linked to xylem architecture (Hacke, 2001).
Trees try to avoid damages caused by water deficits, negotiating carbon uptake capacity and ensuing in a diminution of stored carbohydrates while respiration is continuing (Allen et al., 2010). This has a huge consequence in carbon deficits and, due to the continued metabolic demand for carbohydrates, the plant starves (Klemm, 2019) and the forest, slowly, starts its decline.
This critical physiological situation makes trees more vulnerable to biotic agents, which benefit from the already stressed plants. Additionally, due to a low water potential, the production and translocation of resin start to decrease and this implies a lowering of the defences against insect attacks (i.e. pine processionary moth (*Thaumetopoea pityocampa*)) and consequently, fungi weaken tree vitality (Allen et al., 2010).

Forests growing in particularly cold ecosystems (such as the Alps) are more prone to climate changes, since these kinds of environments represent one of the most sensible terrestrial regions (Körner, 1999). For this reason, these areas can be considered effective indicators even of small change in climate conditions (Rossi et al. 2006), and high-altitude forests can be considered a kind of database to obtain information relating to the past climate trends.
Moreover, an increase in temperature could cause an extension of the thermal zones favourable to the formations of more thermophilic broad-leaved trees, moving these species to higher mountain ranges, currently dominated by micro-thermal conifers; thus, changes in the high altitude forests could alter the delicate role they play in the protection of the slopes from erosion and in defence from avalanches (Mauro, 2017).

Venosta valley is a particular example for studying the correlation between drought and forest die-off: the sheltering effect of surrounding mountains makes the area one of the driest in the Alpine arc (Autonome Provinz Bozen-Südtirol, 2010). Along this valley, human activities like the intense forest exploitation and livestock grazing caused multiple alluvial events, especially in the past, resulting in important damages for the close villages as Silandro and Lasa. Since the erosive and alluvial events'

frequency increased, in 1850 and again in 1950 the forest department of Merano started the afforestation of the south slopes of the Venosta valley, in order to increase the terrain stability: it was one of the biggest afforestation in the area. Around 1200 hectares were planted at the end of 1964 using mainly *Pinus nigra,* since there was a high availability of these seeds at that time (Buscarini et al., 2019).

Nowadays, however, this species, widely used in the past in Venosta valley, is facing a diffused mortality. *Pinus nigra* is generally able to live in harsh environment, but if it is subjected to periods of prolonged drought, it can die for carbon starvation since it usually adopts an isohydric physiological strategy in response to water stress (Forner et al., 2014); in fact, when drought occurred, it has shown a significant vulnerability to embolism with a loss of 50% of hydraulic conductivity (Martin-Benito et al., 2017). This factor makes the species more susceptible to longer and more frequent droughts, affecting the vitality of the forests and therefore its distribution area.

*Pinus nigra* currently covers more than 3.5 million hectares (**Figure 2**), "*is a fast-growing conifer with a wide but fragmented distribution across Europe and Asia Minor, predominantly in mountain areas. It has also become naturalised in some areas in North America"* (Enescu et al., 2016).

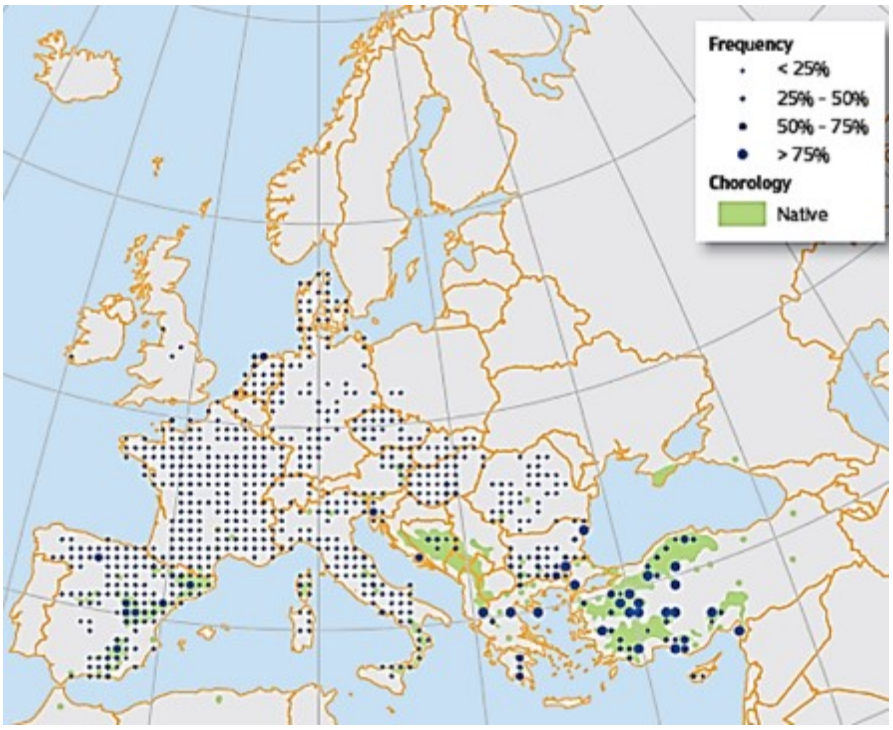


**Figure 2:** *Distribution map for Pinus nigra (Enescu et al., 2016).*

Austrian pine can grow in pure stands or in association with other broad-leaved or conifer species, in particular *Pinus sylvestris*. (Enescu et al., 2016).

Fires may damage Austrian pine stands, altering plant community composition in favour of typical post-fire communities with perennial grass species as well as other tree species such as maritime pine (*Pinus pinaster*), Aleppo pine (*Pinus halepensis*), holm oak (*Quercus ilex*) which are more fire resistant in some of the climatic conditions where Austrian pine lives: "*it regenerates with difficulties after a fire event, particularly during periods with extreme droughts when the development of seedlings can become challenging"* (Enescu et al., 2016).

The future distribution of Austrian pine will likely change considerably as a result of climate warming, but the responses will be different depending on the geographic region: in central Europe changing climate is thought to lead to an expansion, while in the Mediterranean regions climate warming increases water stress and thus has a negative influence on the growth of this species (Enescu et al., 2016) and on the vital state of forests.

## 1.1 Objectives

The main objective of this study is to give new insights on the long-term drought-induced xylem adjustments prior decline and on the triggering process behind trees' drought-induced mortality.

This may also help to understand which are the early-warning signals indicating the specie-specific threshold between survival and mortality.

For this purpose, I investigated the effects of drought in wood anatomical traits of Austrian pine (*P. nigra*) in Venosta valley (Italy). In particular, through a dendro-anatomical approach, I aimed to identify the differences in xylem traits between the *non-declining trees (ND)* and the *declining trees (D)* of *Pinus nigra.*

The specific objectives are:

- understanding what are the xylem adjustments induced by drought;
- highlighting the potential intra-specific differences in xylem traits between *declining* and *non-declining trees*;
- improving the prediction of individuals' mortality identifying which are the declining signals prior mortality.

This kind of information may be useful in (I) the selection of future strategies of forest management, (II) the identification of models to predict the geographical distribution and vitality of plant communities and (III) the selection of indicators for past drought events which may help for climate reconstruction.

# 2) MATERIALS AND METHODS

## 2.1 Study site and climate

The study area is located at 1100 m a.s.l. on south slope (6.7% s.l.p.) above Lasa village in Venosta valley (46°37'55.7"N, 10°40'18.9"E), which is placed in Alto Adige region (Italy) (**Figure 3 and Figure 4**). The watershed is characterized by Adige torrent, which crosses the valley as far as Bolzano and it drains a catchment area of approximately 2700 km²; for this reason, especially in the middle and lower Venosta, there are extensive fruit crops, while vegetable crops are widespread in the upper part of the valley (Autorità di bacino nazionale del fiume Adige, 2022).

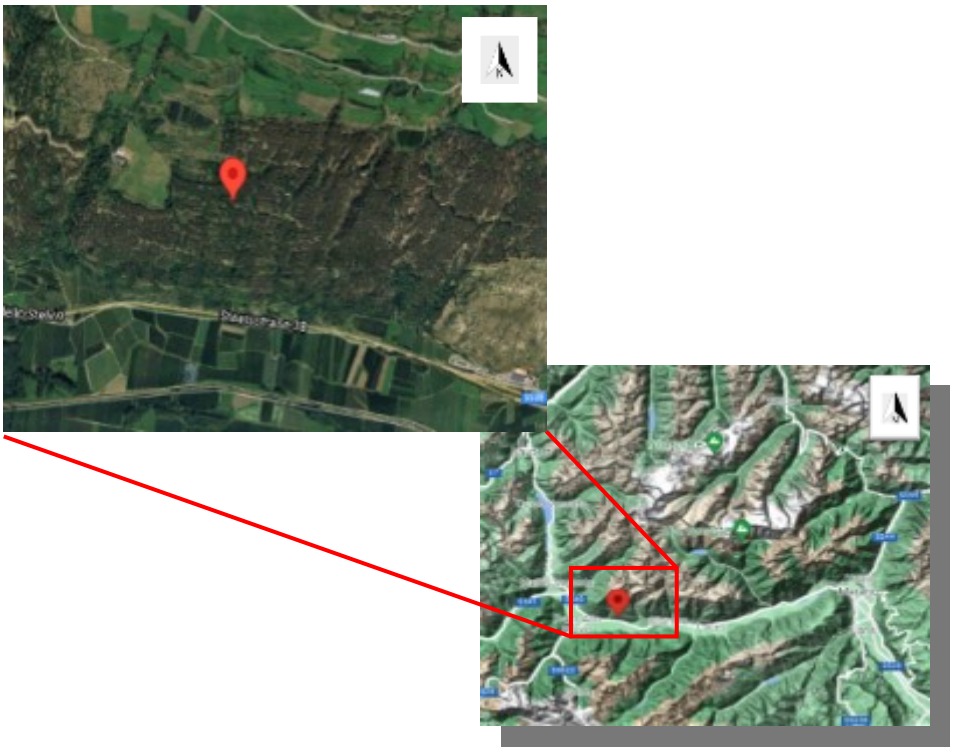

**Figure 3:** *Images of the study site realized with Google Maps using the geographic coordinates. (Personal elaboration).*

**Figure 4:** *Overview of the forest die-off in the study site.*

Venosta valley has the lowest percentage of rainfalls and the highest temperatures in the entire Alpine arc. (N.p., "Flora e fauna della Val Venosta in Alto Adige. Tutta la diversità delle Alpi in una valle". *Venosta.net,* (n.d)).

Both temperature and precipitation follow a bell shape with a single summer peak. Maximum precipitation is reached in August with ca. 70 mm, (**Figure 5**), while the driest periods between December and April, with January having in average just 20 mm. The minimum mean monthly temperatures ($T_{min}$) during winter reach ca. -3 °C, while the maximum mean monthly temperatures ($T_{max}$) during summer reach almost 30°C (**Figure 5**).

Due to low precipitation and strong solar radiations and to south exposure of the slope, vegetation has to cope with extreme drought conditions (Autonome Provinz Bozen-Südtirol, 2010).

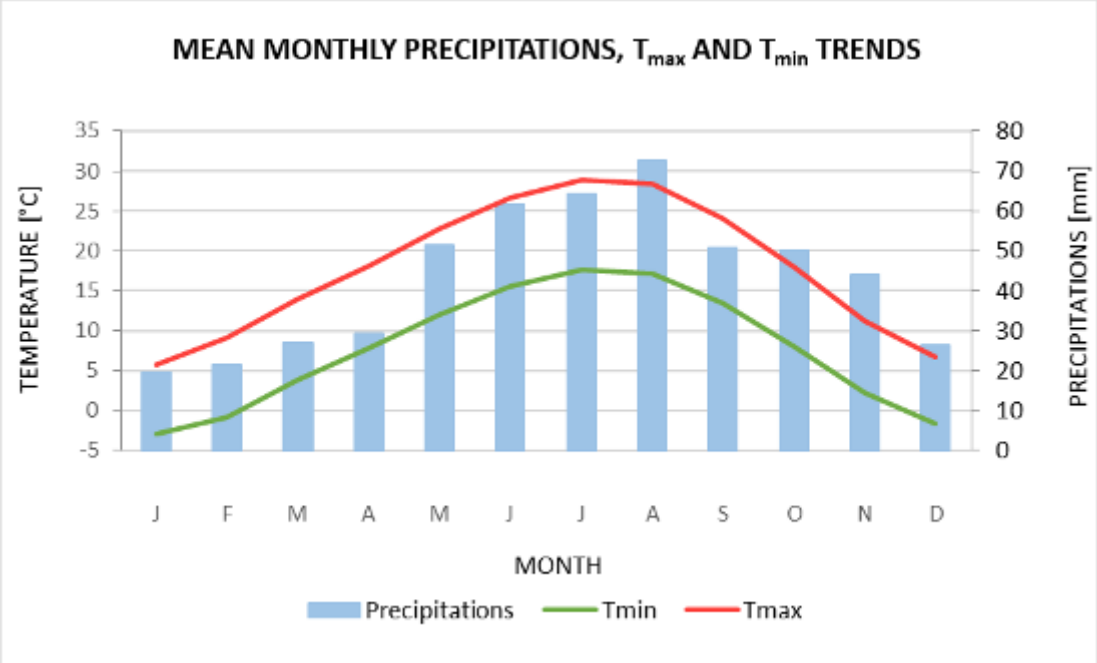


**Figure 5:** *Distribution of mean monthly precipitation and temperatures during the year referred to the 1901-2020 period. The climatic data refer to the coordinates of the study site and were provided by CNR-ISAC (Bologna, IT; Brunetti et al., 2004, 2006).*

Regarding the trends of Venosta valley, minimum and maximum mean annual temperatures increased of ca. 2°C from 1901 to 2020. On the other hand, the distribution of annual precipitations during the same time-span (1901- 2020) seems to have less evident variation, in fact it increased of just ca. 7 mm in ca. 120 years (**Figure 6**). Therefore, the rise of temperatures seems not to be counterbalanced by precipitations trend, signal that may indicate an increasing evaporation with the consequence of more frequent drought events.

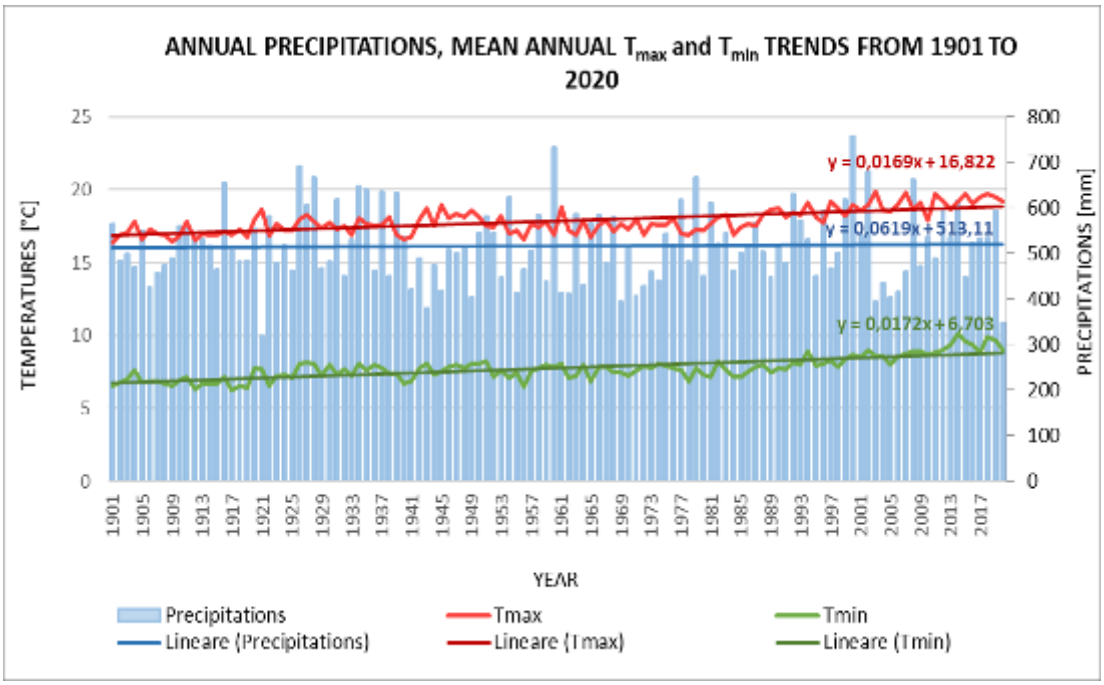


**Figure 6:** *Annual precipitations and mean annual temperatures from 1901 to 2020. The climatic data refer to the coordinates of the study site and were provided by CNR-ISAC (Bologna, IT; Brunetti et al., 2004, 2006).*

If we look at the same timespan (1091-2020), but taking into consideration the vegetative period, roughly from April to September, the increase in temperatures ($T_{max}$ and $T_{min}$) is still very clear and just slightly higher than the yearly one (**Figure 7**). In fact, the increase in this case is of ca. 2.1 °C. Instead, precipitation sum of the April-September period increased of just ca. 13mm. Therefore, focusing on the growing season, temperature seem to show a slightly steeper increase than precipitation one.

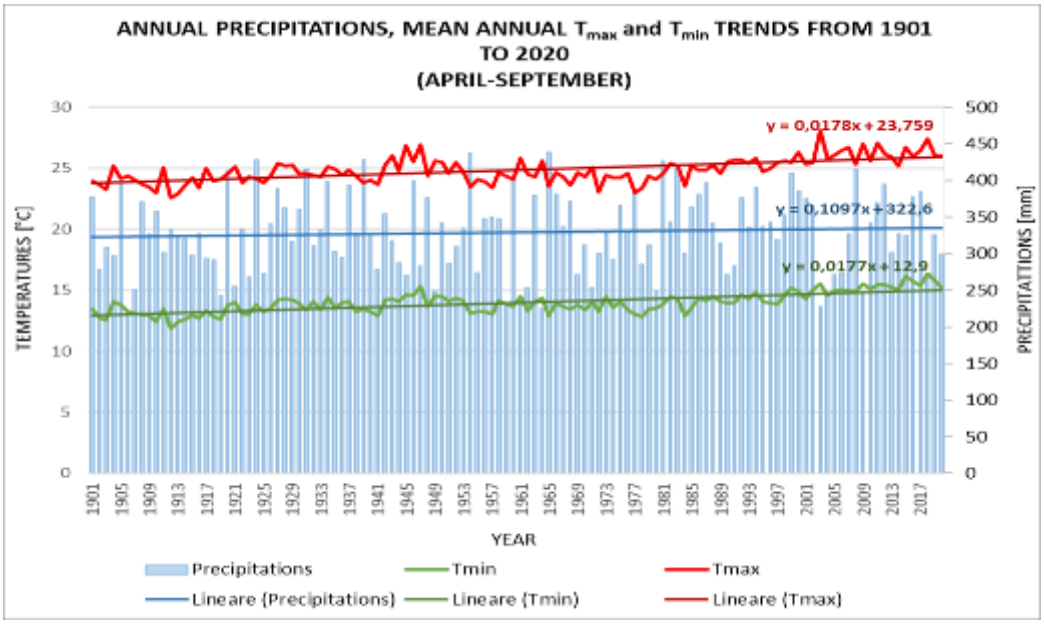


**Figure 7:** *April-September precipitation sums and mean annual temperatures from 1901 to 2020. The climatic data refer to the coordinates of the study site and were provided by CNR-ISAC (Bologna, IT; Brunetti et al., 2004, 2006).*

Another significant element to describe climate conditions is the mean annual Standardised Precipitation-Evapotranspiration Index (SPEI) that detects, monitors and analyses drought according to their intensity and duration (Vicente-Serrano et al., 2010). SPEI is based on the monthly difference between precipitation and evapotranspiration. Therefore, I used the SPEI with cumulated data of 3 months. This index in general has a value that oscillates between 2 and -2: the positive values indicate normal-humid climate situations, while negative values represent dry climatic condition.

Looking at SPEI-3 trend over years (**Figure 8**), it is possible to see that precipitations may have been progressively less capable to contribute to the recharge of the aquifers due to high temperatures and therefore high rates of evapotranspiration (Mariani et al., 2018). In fact, SPEI-3 changed, considering the linear trend, from 0.2 to -0.1 in ca. 120 years. Furthermore, during the growing season (April-September) SPEI-3 trend line has a less evident slope, but still slightly decreasing (**Figure 9**).

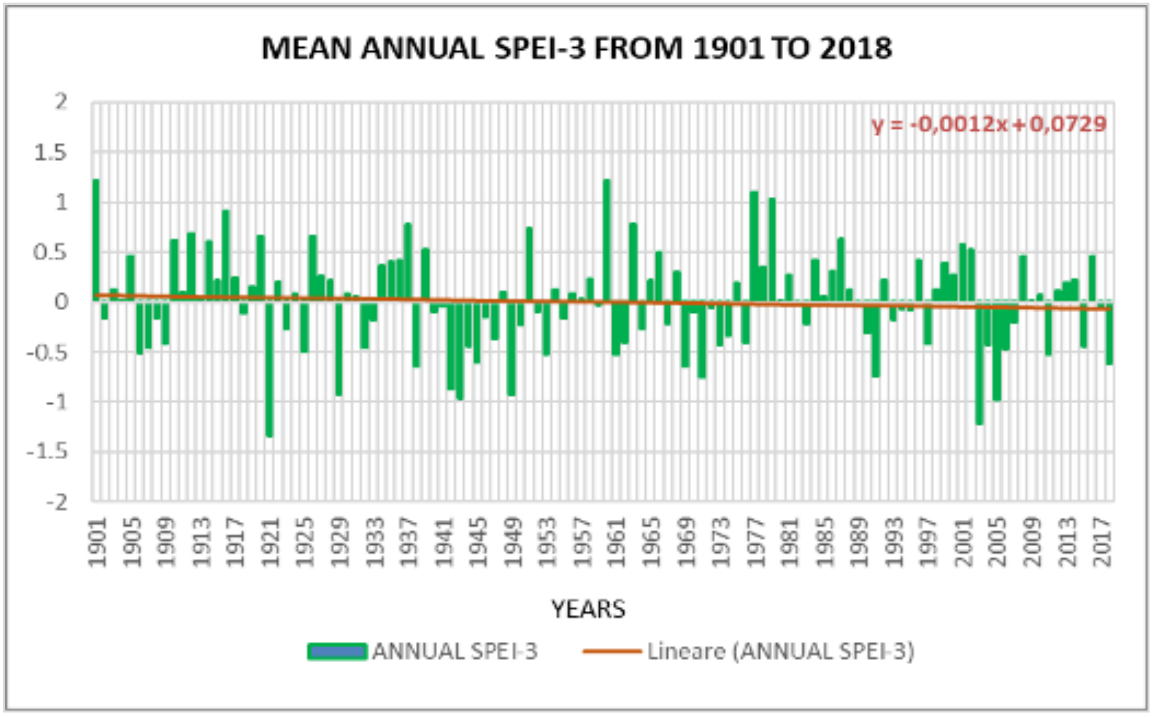


**Figure 8:** *Time series of SPEI-3 from 1901 to 2018. The SPEI data refer to the coordinates of the study site and were provided by CNR-ISAC (Bologna, IT; Brunetti et al., 2004, 2006).*

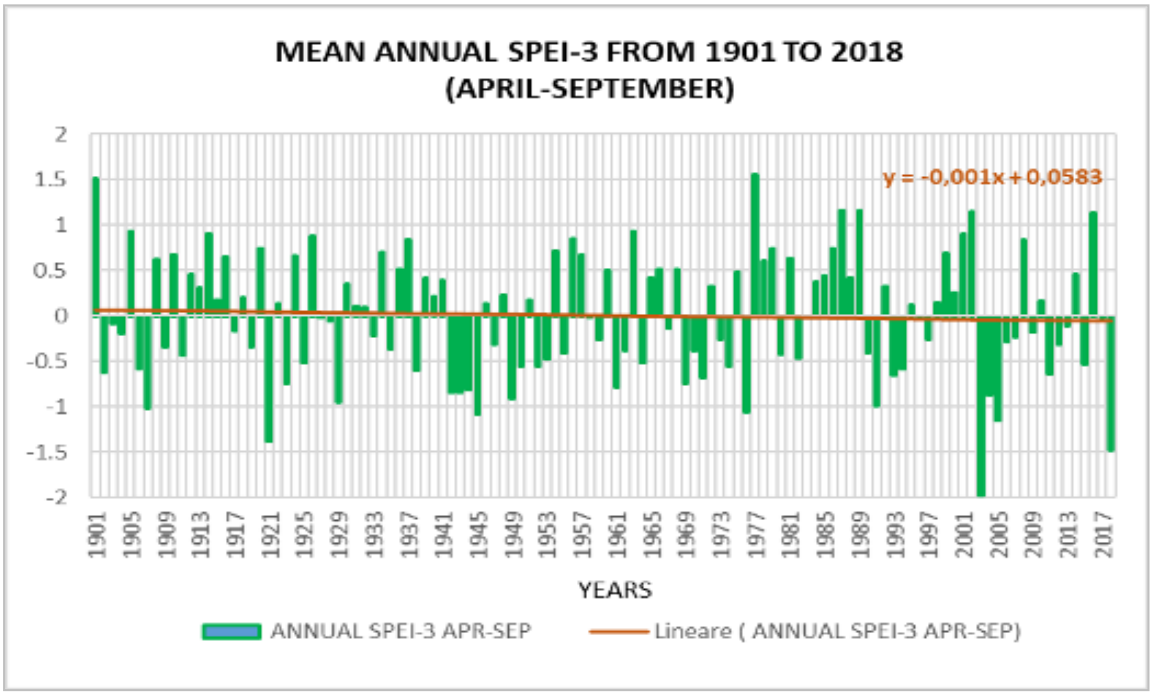


**Figure 9:** *Time series of SPEI-3 from 1901 to 2018 during April-September period. The SPEI data refer to the coordinates of the study site and were provided by CNR-ISAC (Bologna, IT; Brunetti et al., 2004, 2006).*

## 2.2 Sampling method

In 2019, the members of the Tesaf ecological research group joined forest operations of the Bolzano Province Forest Service, during which operators cut basal section (ca. 1 m above root collar) of selected trees. Sampled individuals had all similar height (ca. 15 m), similar microsite and competition conditions and were even-aged. Log sections were collected from both *non-declining (ND)* and *declining (D)* Austrian pines (*Pinus nigra*) (**Figure 10**), growing one close to the other, on the base of canopy status: 9 sampled with a vigorous crown were selected for the group of *ND* trees and 8 sampled with brownish crown for the group of *D* trees.

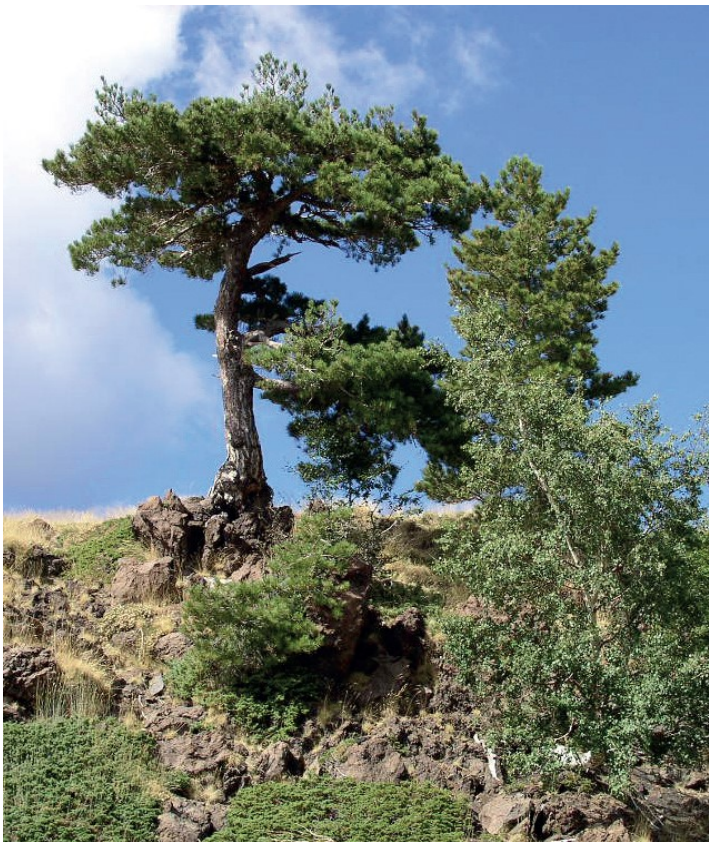

**Figure 10:** *Pinus nigra (Enescu et al., 2016).*

## 2.3 Laboratory analysis

### *2.3.1 Preparation of samples and measurement of growth rings*

Once brought in the laboratory, one slat per tree was cut from bark to pith, paying attention to follow perpendicular direction respect to rings and avoiding any evident defect. Then, it was possible to proceed with the smoothing of the transversal surface, to measure and crossdate ring widths to obtain a master chronology of *ND* and *D* plants. The polishing of the slats was done manually with increasingly fine-grained abrasive papers. Once obtained a smooth surface, it was possible to measure the accretions using a special device consisting of:

- A sliding plane (CCTRMD: Computer Controlled Tree Ring Measuring Device, (Aniol, 1987))
- A binocular stereoscope with magnifications from 6 to 60X.
- A software that manages the acquisition of data sent by the CCTRMD to the computer: CATRAS (Aniol, 1983).

The various values of the annular amplitudes were recorded trough CATRAS software (Aniol,1983) with a precision of 0.01 mm, thus obtaining the measurements of the annual series for each individual core.
After this, we checked dating of our samples through COFECHA program (Grissino-Mayer 2001) and finally we selected 10 samples for the quantitative wood anatomy assessment (5 from *ND* group and 5 from *D* one) on the base of absence cross-dating issues or visible defects.

### *2.3.2 Preparation of the microscopic sections*

The second step was related to the preparation of slides for quantitative wood anatomy assessment.
The woody slats were divided into further transversal pieces from bark to pith, around 4-5 cm long. To limit cell breakdown in the cutting step, the samples were

hydrated for at least 10-15 minutes. A fixed blade rotary microtome (Leica RM 2145) was used to create the sections of 12 μm thickness.

The cuts are performed with the woody sections arranged vertically and with the fibres directed at 90 ° with respect to the blade. A solution of water and alcohol with a concentration of 50% was used as the lubricating liquid to facilitate the displacement of the section on the slide.

### *2.3.3 Samples fixation and staining*

The staining and fixing procedure consists of four steps: bleaching, staining, dehydration, and slide mounting. The bleaching was done by applying a few drops of bleach for 10 minutes. The sample was then rinsed with distilled water and stained. The sections were coloured to increase the contrast between the cell spaces and the walls. The staining was done using safranin (1% in distilled water), applying a few drops for at least 15 minutes on the samples: in this way, all lignified structures were red coloured. Therefore, three rinses were carried out: the first with distilled water only, the second with a solution of 50% alcohol and 50% water and the third with alcohol at 98%.

Subsequently, the samples were further dried with a cloth and fixed to the slide using *Eukitt* medium (BiOptica, Milan, Italy), with a refractive index similar to that of the slide (n = 1.51-1.54). The medium applied to fix the slide needs at least 24 hours to dry and to prevent the slide cover from moving during this phase.

## 2.4 Images capturing and elaboration

To obtain microscopic digital images, we used a slide scanner *Nikon D-Sight*, available at the MAPS Department of University of Padova (Medicina Animale, Produzioni e Salute) with a magnification of 40x.

Digital images were then analysed through *ROXAS* software that is a macro of the *Image-Pro Plus* software and basically is an image analysis tool designed to analyse the xylem structures in cross-sectional view of trees (angiosperms and conifers), shrubs and herbaceous plants. It is based on the image processing and analysis capabilities of *Image-Pro Plus* and can interacts with *MS Excel* for data outputs.

The first time the image is loaded, *ROXAS* requires the creation of a calibration: in our case the value for the calibration selection was 1.9936 Pixel/Unit.

The next step is manual acquisition of the AOI (Area of Interest), to select portions of images to be analysed. At this point, it is really important to select equal portions of latewood and earlywood within the same ring in the AOI, in order to not influence the correct calculation of the mean size of the cells in a given year (**Figure 11**).

After that, we started with the *Batch Run Project* phase, during which *ROXAS* makes the automatic analysis.

Then there's the need to perform manual editing to mark annual rings and correct potential errors in the cells identification. Then crossdating of every single image is performed, referring to the *D* and *ND* master chronologies.

At the end of all these steps, *ROXAS* realized an *Excel* outputs for each image, in which all anatomical parameters are referred to the exact year. Lastly, through summary-output function, *ROXAS* gave as output the dated anatomical series of every individual, merging the different microscopic images together.

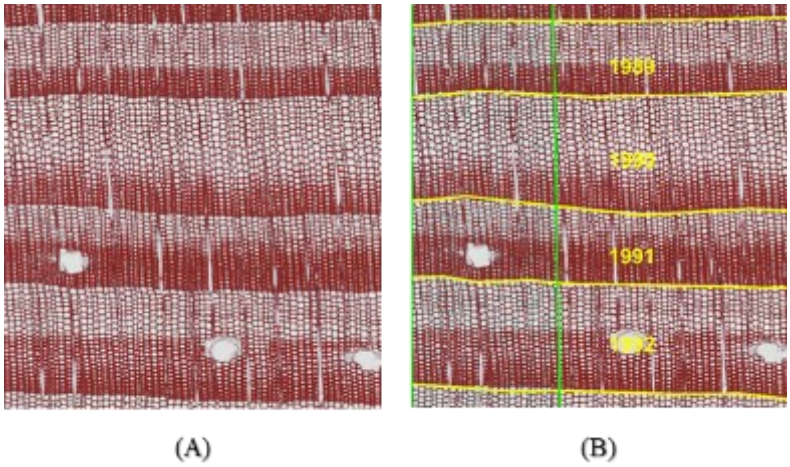


**Figure 11:** *Cut-out image of the evaluated cross-section of Pinus nigra during ROXAS processing:* **(A)** *Original image;* **(B)** *AOI defined in green and ring borders manually added and correctly dated after cross-dating highlighted in yellow.*

For the following analyses we selected these parameters:

- **Mean ring width (MRW, [µm])**, the yearly average width of the ring;
- **Cells number (CNo)**, the yearly sums of all the conduits;
- **Cell lumen area at 50° percentile (LA 50%, [µm$^2$])**;
- **Tangential cell wall thickness (CWTtan, [µm])**, the mean thickness of tangential cell walls;
- **Mean hydraulic diameter (Dh, [µm]),** is the sum (cell hydraulic diameter ^5) / sum (cell hydraulic diameter ^4);
- **Theoretical hydraulic conductivity (Kh, [m4*s-1*MPa-1])** as approximated by Poiseuille's law and adjusted to elliptical tubes.

## 2.5 Data analysis

To remove the typical age-related trends of anatomical parameters (Carrer et al., 2015; Cook, 1990), chronologies were standardized using smoothing spline with 50% frequency cut off of 30 years, through *R* software (Team, 2013). Standardized series were subsequently mediated to build mean chronologies for all the anatomical parameters studied representative of D and ND groups, by averaging corresponding individuals.

From this new standardized anatomical series, I created several graphs of each parameter considered for *declining* and *non-declining* trees to create a clear comparison between two groups.

After this step, in order to understand if there were statistically significant difference between the means of the *D-ND* trees, I made on *Excel* a T-test for two-samples assuming equal variances on raw anatomical parameters aligning series to cambial age instead of calendar year: looking at the p-value it has been possible to identify which parameters were significantly different. When P-value is lower than the significance level (in our case set at 0.05) we can conclude that the difference between the two means is not equal to 0.

The final step of data analysis was to see the correlation between the standardized anatomical parameters and the daily climatic data, in order to understand whether the two groups featured a different sensitivity in their anatomical traits respect to climate. To make this last phase I worked with *Excel*: through *Pearson correlation* formula it had been possible to find out the correlation coefficients for each detrended anatomical parameter with the climatic parameters ($T_{max}$, precipitations and SPEI-3) then, I build graphs showing such correlations. Critical value of Pearson correlation was 0.2, according to number of observation and significance level.

# 3) RESULTS

## 3.1 Anatomical series

The period covered by the anatomical series, obtained from *non-declining* (*ND*) and *declining* (*D*) samples, goes from 1942 to 2016. The oldest plants belong to the *ND* group, while the samples from *D* group are slightly younger: the two oldest samples (*ND*) start from 1942, the youngest one (*D*) from 1950.

The results obtained from the first part of the analysis are the raw anatomical series for the selected parameters aligned with years (1942-2016) and with age (1-75) of the *D* and *ND* trees. Since the analysed trees have more or less the same age, the raw series are useful to highlight potential different growth trends between *D* and *ND* trees.

In the following page there's an example of the comparison between the raw years-age graphs obtained for the CNo (**Figure 12**) (All the other raw anatomical series for years and age are available in the **Annex 1**).

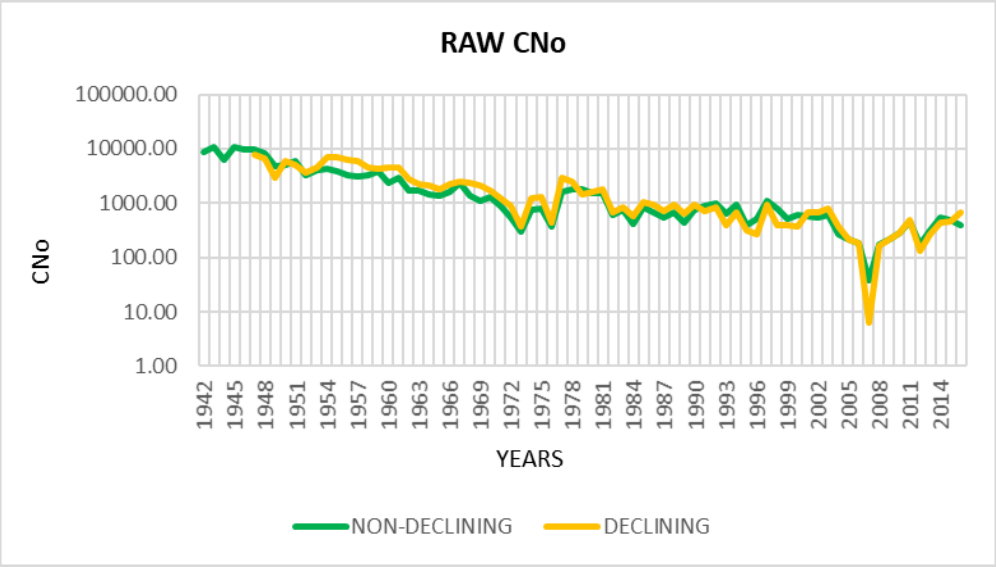


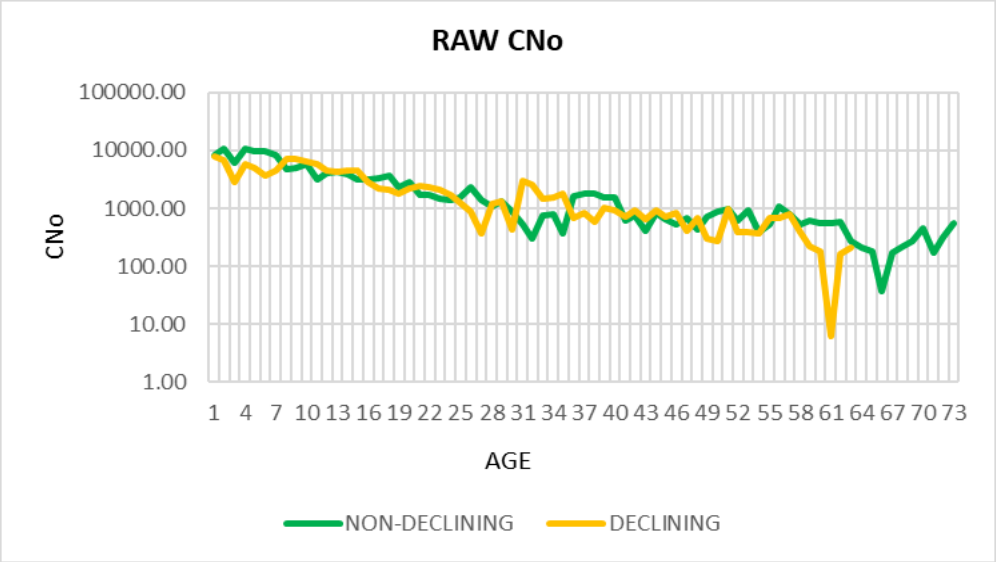


**Figure 12:** *Above: raw cell number (CNo) series of declining and non-declining trees aligned with calendar year; below: raw cell number (CNo) series of declining and non-declining trees aligned with cambial age. The logarithmic scale has been used for both, raw series.*

As we can see from the two graphs, the trends of the two groups are identical. However, aligning series with cambial age, it is possible to compare the ontogenetic trend of the two groups.

Considering raw anatomical series aligned with age, I obtained a table (**Table 1**) in which it is possible to see the mean values and the standard deviation for each parameter of *declining* and *non-declining* trees. In this case the only statistically significant parameter (identified through the T-test) is the tangential cell wall thickness (CWTtan; **Table 2**).

| *Pinus nigra* | DECLINING | NON-DECLINING |
|---|---|---|
| N°of trees | 5 | 5 |
| MRW [µm] | 1174.10 ± 912.61 | 1325.86 ± 1081.00 |
| CNo | 1932.25 ± 2049.83 | 2104.06 ± 2648.67 |
| Dh [µm] | 25.96 ± 4.50 | 25.63 ± 4.45 |
| Kh [m4*s-1*MPa-1] | 7.34E-09 ± 6.09E-09 | 6.45E-09 ± 4.46E-09 |
| CTWtan [µm] | 4.21 ± 0.63 | 4.44 ± 0.69 |
| LA50% [µm2] | 254.56 ± 104.17 | 228.41 ± 91.56 |

**Table 1:** *Mean values and standard deviations of anatomical parameters. The data used are the raw anatomical series aligned with age and created by ROXAS.*

| | *MRW* | *CNo* | *Dh* | *Kh* | *CWTtan* | *LA50%* |
|---|---|---|---|---|---|---|
| P(T<=t) two tails | 0.364 | 0.664 | 0.658 | 0.311 | 0.038 | 0.110 |

**Table 2:** *P-values obtained by T-tests for each anatomical parameter. The highlighted p-value of CWTtan is minor than the significance level (in this case set at 0.05).*

Through the standardization of the raw series, I gained the detrended anatomical series aligned with years for each parameter. These data are useful in the search for climatic correlation because they are not influenced by intrinsic ontogenetic trend.
In the following pages some examples of the standardized anatomical series aligned with years are presented (all the other detrended series are available in **Annex 2**).

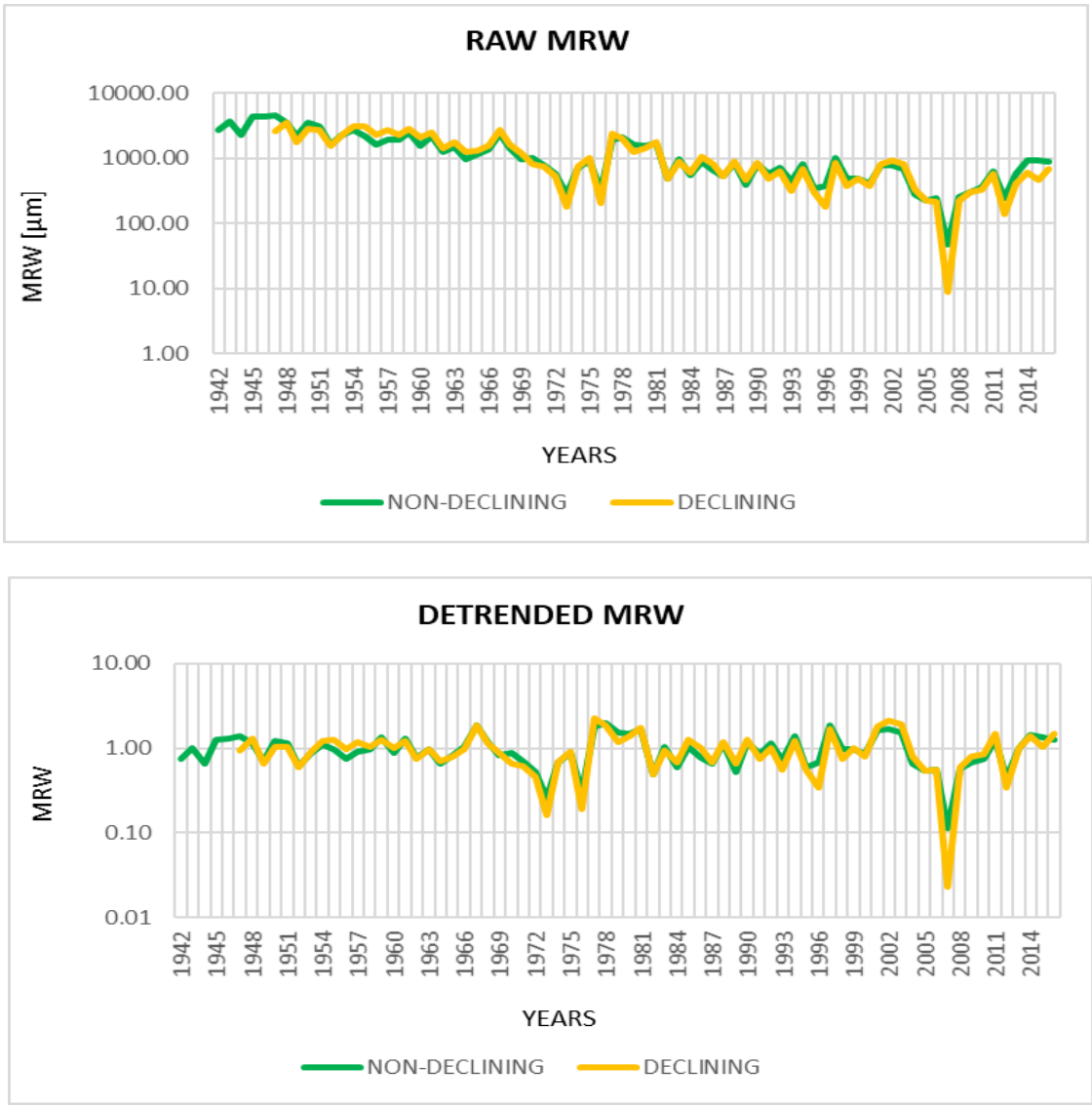


**Figure 13:** *Above: raw mean ring width (MRW) series of declining and non-declining trees aligned with calendar year; below: detrended MRW series of declining and non-declining trees aligned with years. The logarithmic scale has been used for both, raw and detrended series.*

The two series are similar, there are not substantial differences, but there's an evident differentiation in 2007 (**Figure 13**).

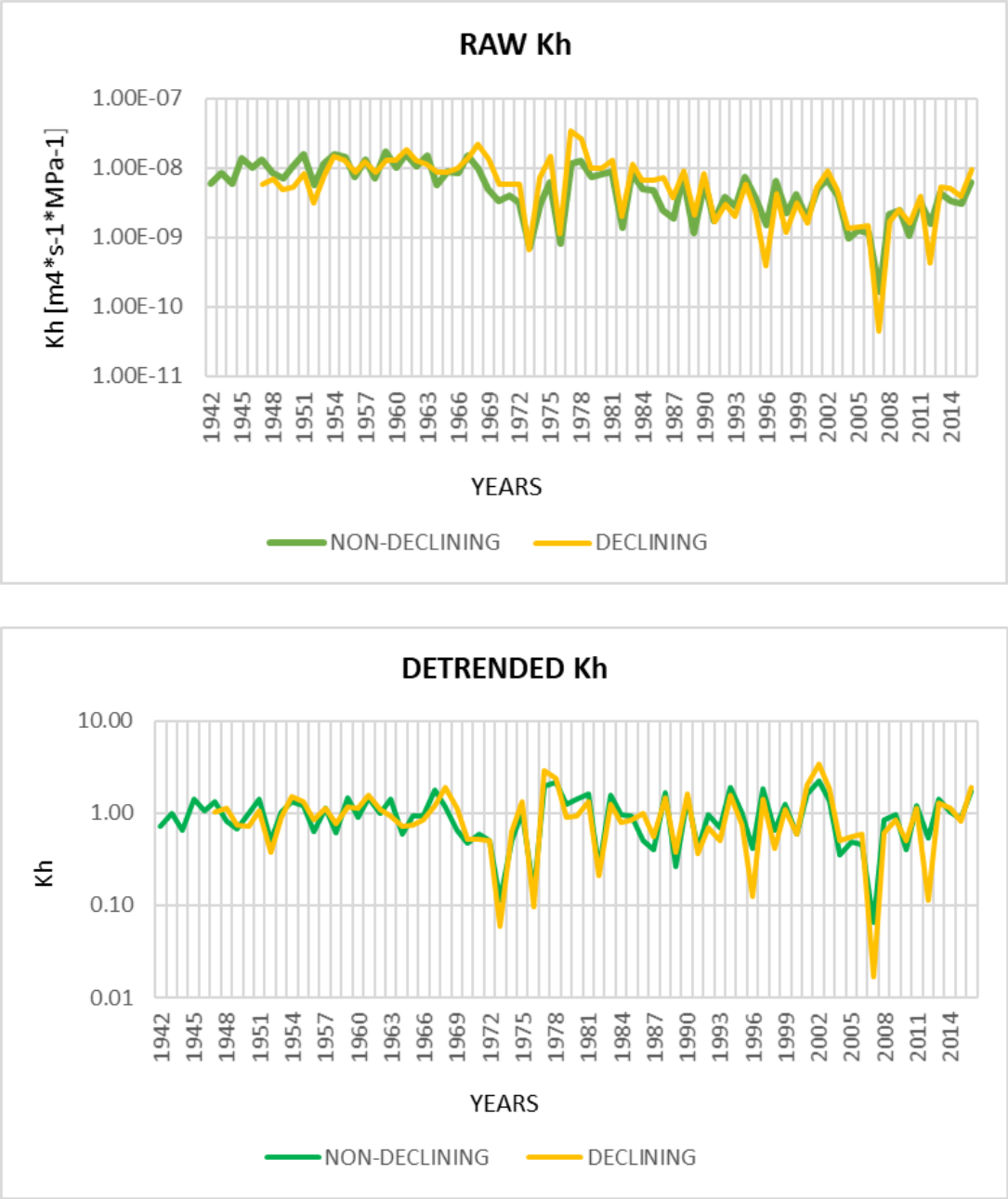


**Figure 14:** *Above: raw theoretical hydraulic conductivity (Kh) series of declining and non-declining trees aligned with calendar year; below: detrended Kh series of declining and non-declining trees aligned with years. The logarithmic scale has been used for both, raw and detrended series.*

The two trials follow more or less a similar trend, there are not significance differences, but looking at the detrended series, it is possible to see evident differentiations in1996, 2007 and 2012 (**Figure 14**).

## 3.3 Climate-variables correlations

From the climate-anatomical traits correlation, I obtained associations between anatomical traits and maximum temperature, precipitation and SPEI-3. The considered timespan refers to the years of the anatomical series: 1942-2016 for the *non-declining* trees and 1947-2016 for the *declining* ones. The results divided according to the anatomical traits analysed are presented below.

### a) MRW: Mean ring width

MRW resulted significantly correlated to precipitations and SPEI-3 between late-spring to early-summer (Table 3; Figure 16; Figure 17), while maximum temperature did not seem to influence radial growth (Table 3; Figure 15).

| | | Pearson correlation | | | | | | | |
|---|---|---|---|---|---|---|---|---|---|
| | | A | M | J | J | A | S | apr-set | year |
| Tmax | D | -0.12 | -0.08 | -0.09 | -0.18 | 0.03 | 0.13 | -0.09 | 0.03 |
| | ND | -0.06 | -0.09 | -0.04 | -0.11 | 0.06 | 0.16 | -0.02 | 0.07 |
| PREC | D | -0.04 | 0.26 | 0.23 | 0.03 | -0.03 | -0.19 | 0.10 | 0.17 |
| | ND | -0.06 | 0.23 | 0.23 | 0.02 | -0.04 | -0.18 | 0.07 | 0.18 |
| SPEI-3 | D | 0.21 | 0.25 | 0.21 | 0.36 | 0.16 | -0.06 | 0.28 | 0.23 |
| | ND | 0.20 | 0.24 | 0.16 | 0.25 | 0.08 | -0.11 | 0.20 | 0.21 |

**Table 3:** *Climate-MRW Pearson correlation matrix. The data used are the detrended anatomical series of D and ND trees. The values highlighted are significant.*

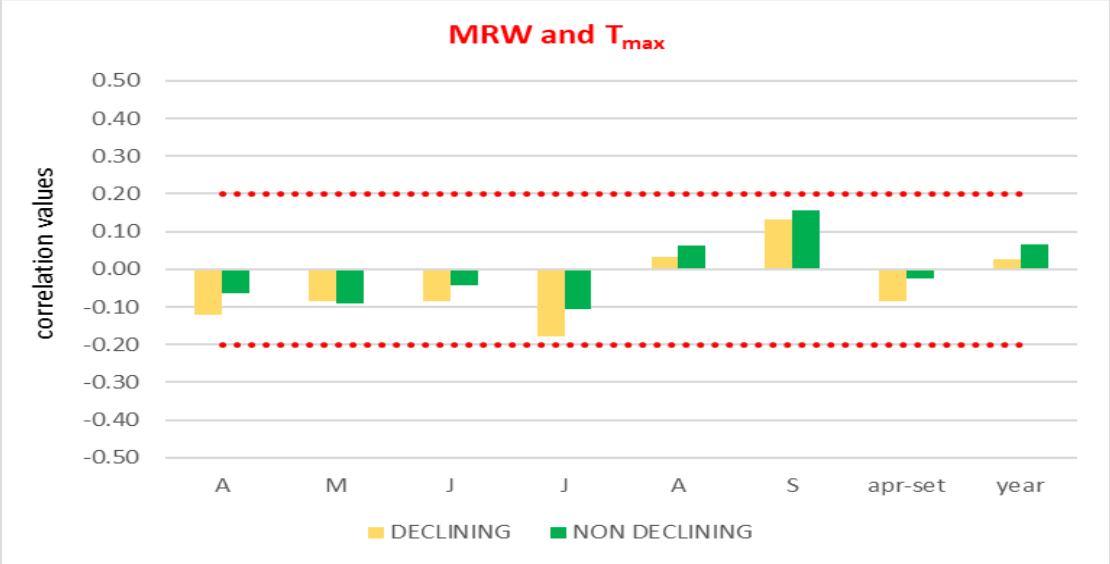


**Figure 15:** *Correlation between Tmax and detrended MRW (mean ring width) for declining (D) and non-declining (ND) series. The dashed red lines are the 0.05 significance thresholds.*

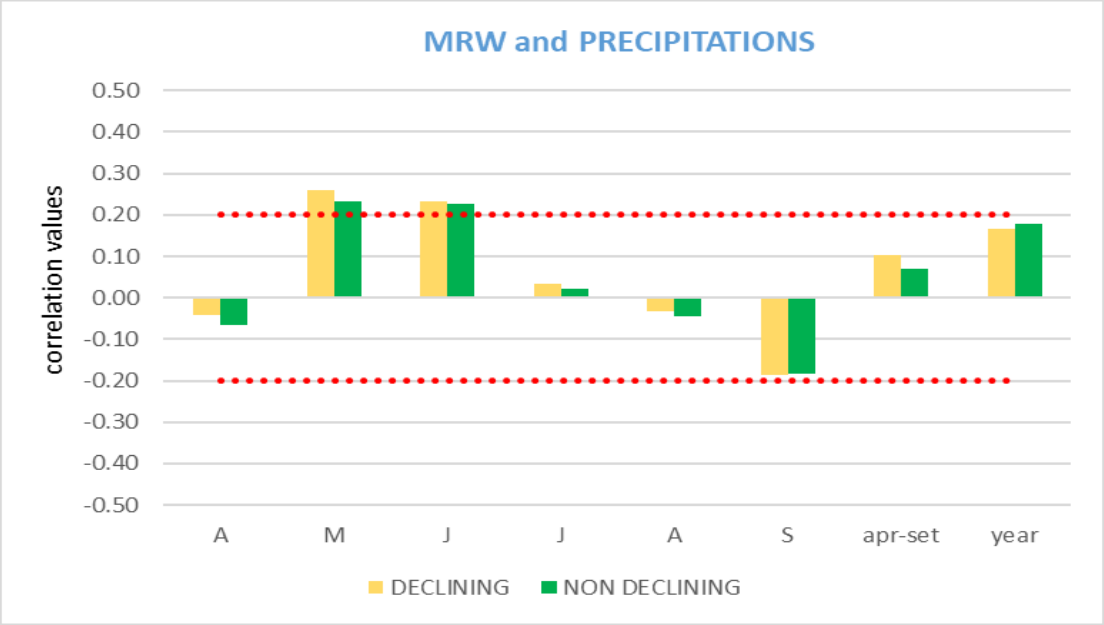


**Figure 16:** *Correlation between precipitations and detrended MRW (mean ring width) for declining (D) and non-declining (ND) series. The dashed red lines are the 0.05 significance thresholds.*

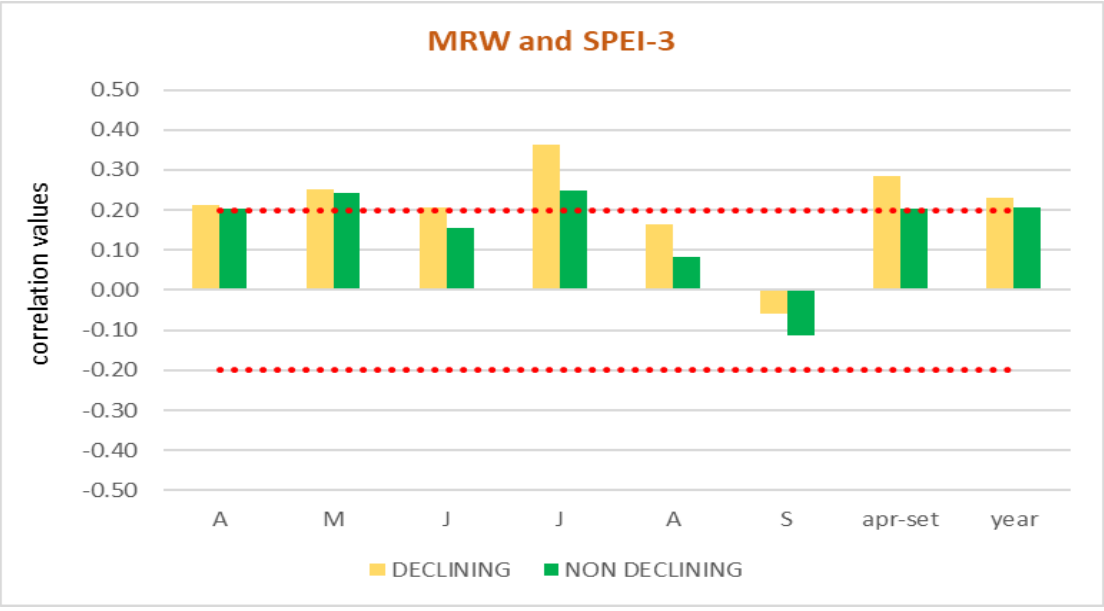


**Figure 17:** *Correlation between SPEI-3 and detrended MRW (mean ring width) for declining (D) and non-declining (ND) series. The dashed red lines are the 0.05 significance thresholds.*

### b) CNo: Cells number

CNo resulted significantly correlated to temperatures, precipitations and SPEI-3 especially during summer. (Table 4; Figure 18; Figure 19; Figure 20).

| | | Pearson correlation | | | | | | | |
|---|---|---|---|---|---|---|---|---|---|
| | | A | M | J | J | A | S | apr-set | year |
| Tmax | D | -0.16 | -0.08 | -0.09 | -0.20 | 0.10 | 0.20 | -0.06 | 0.00 |
| | ND | -0.06 | -0.08 | -0.04 | -0.17 | 0.10 | 0.23 | 0.00 | 0.06 |
| PREC | D | -0.07 | 0.19 | 0.31 | 0.03 | -0.08 | -0.22 | 0.04 | 0.10 |
| | ND | -0.09 | 0.10 | 0.22 | 0.05 | -0.06 | -0.12 | 0.03 | 0.18 |
| SPEI-3 | D | 0.20 | 0.17 | 0.17 | 0.34 | 0.15 | -0.12 | 0.23 | 0.16 |
| | ND | 0.12 | 0.15 | 0.06 | 0.19 | 0.07 | -0.11 | 0.11 | 0.16 |

**Table 4:** *Climate-CNo Pearson correlation matrix. The data used are the detrended anatomical series of D and ND trees. The dashed red lines are the 0.05 significance thresholds.*

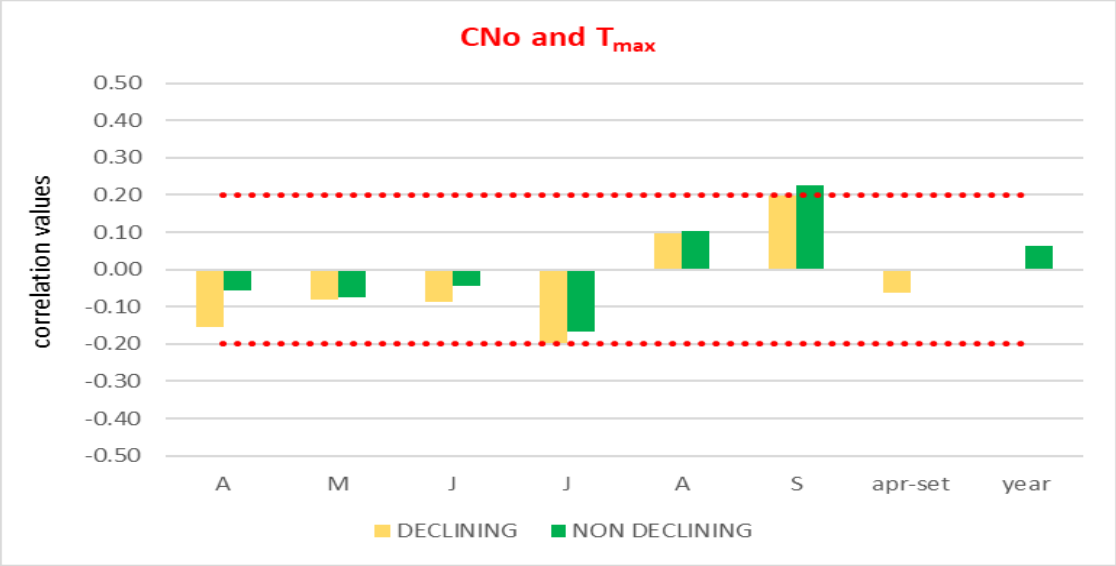


**Figure 18:** *Correlation between Tmax and detrended CNo (cells number) for declining (D) and non-declining (ND) series. The dashed red lines are the 0.05 significance thresholds.*

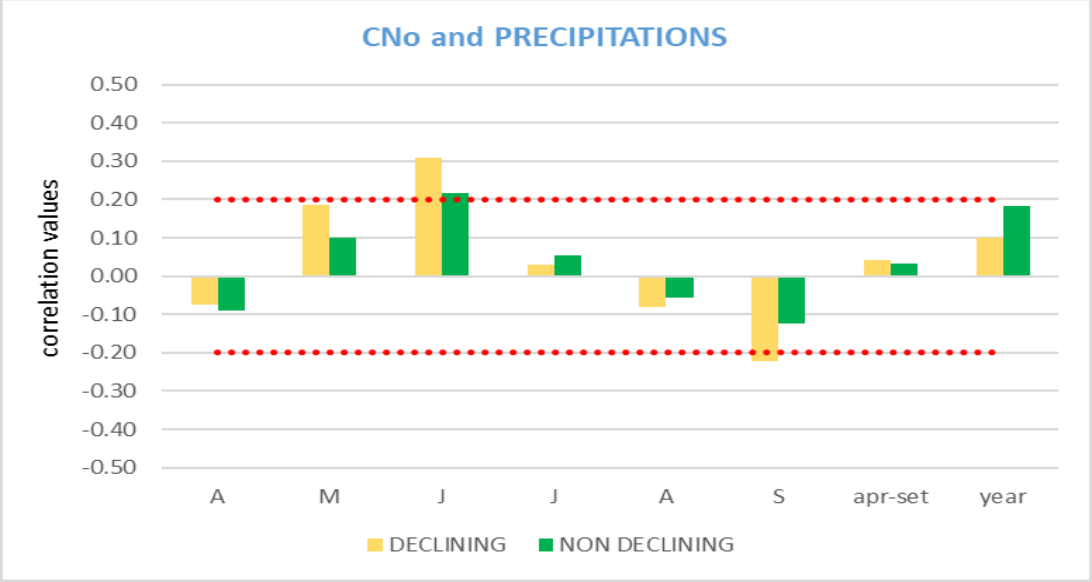


**Figure 19:** *Correlation between precipitations and detrended CNo (cells number) for declining (D) and non-declining (ND) series. The dashed red lines are the 0.05 significance thresholds.*

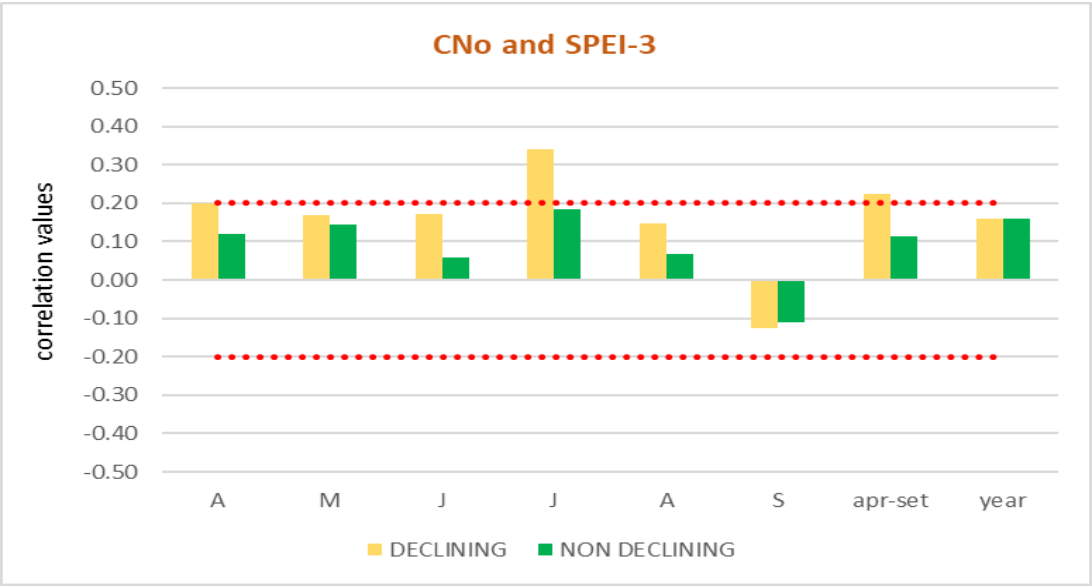


**Figure 20:** *Correlation between SPEI-3 and detrended CNo (cells number) for declining (D) and non-declining (ND) series. The dashed red lines are the 0.05 significance thresholds.*

### c) Dh: mean hydraulic diameter

Dh resulted significantly correlated to temperatures, precipitations and SPEI-3 between spring to early-summer (Table 5; Figure 21; Figure 22; Figure 23).

| | | Pearson correlation | | | | | | | |
|---|---|---|---|---|---|---|---|---|---|
| | | A | M | J | J | A | S | apr-set | year |
| Tmax | D | 0.02 | -0.23 | -0.23 | -0.02 | -0.08 | 0.05 | -0.14 | -0.05 |
| | ND | -0.01 | -0.21 | -0.16 | 0.04 | -0.05 | -0.04 | -0.12 | -0.07 |
| PREC | D | 0.05 | 0.44 | 0.08 | -0.17 | -0.01 | -0.09 | 0.15 | 0.10 |
| | ND | 0.06 | 0.39 | 0.06 | -0.07 | -0.06 | -0.02 | 0.17 | 0.14 |
| SPEI-3 | D | 0.34 | 0.49 | 0.43 | 0.30 | 0.02 | -0.07 | 0.38 | 0.24 |
| | ND | 0.28 | 0.45 | 0.37 | 0.25 | 0.00 | -0.03 | 0.33 | 0.26 |

**Table 5:** *Climate-Dh Pearson correlation matrix. The data used are the detrended anatomical series of D and ND trees. The values highlighted are significant.*

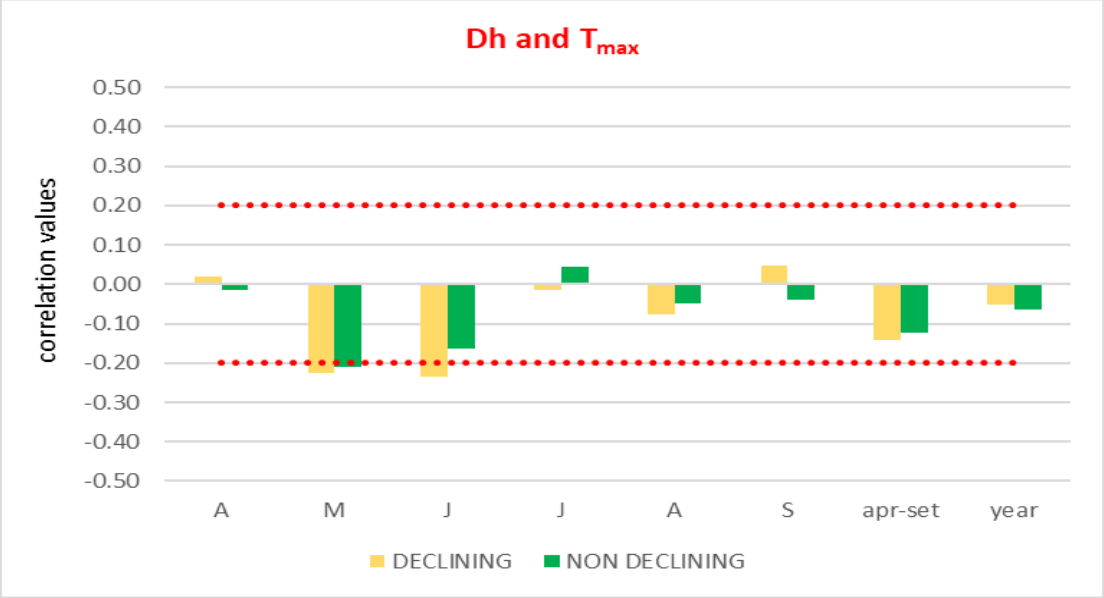


**Figure 21:** *Correlation between Tmax and detrended Dh (mean hydraulic diameter) for declining (D) and non-declining (ND) series. The dashed red lines are the 0.05 significance thresholds.*

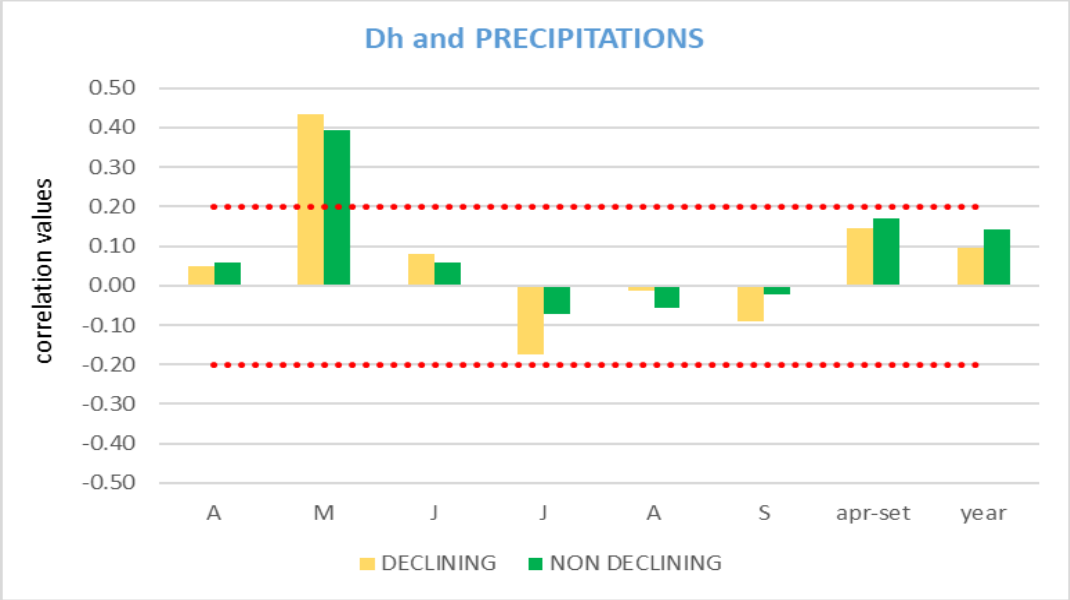


**Figure 22:** *Correlation between precipitations and detrended Dh (mean hydraulic diameter) for declining (D) and non-declining (ND) series. The dashed red lines are the 0.05 significance thresholds.*

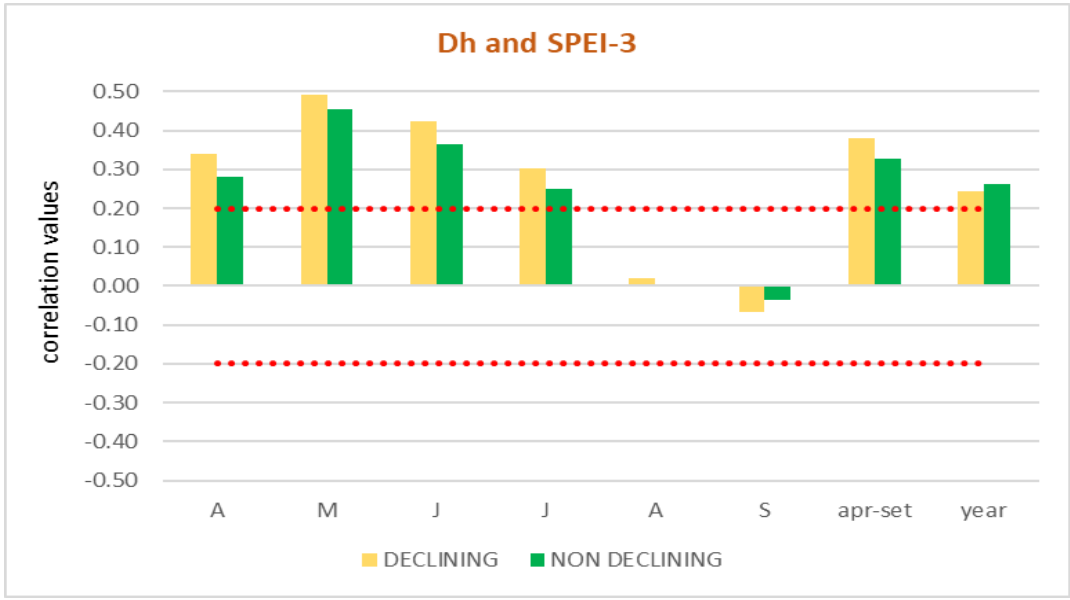


**Figure 23:** *Correlation between SPEI-3 and detrended Dh (mean hydraulic diameter) for declining (D) and non-declining (ND) series. The dashed red lines are the 0.05 significance thresholds.*

### d) Kh: theoretical hydraulic conductivity

Kh resulted significantly correlated to precipitations and SPEI-3 between spring to early-summer (Table 6; Figure 25; Figure 26), while maximum temperature resulted to not influence radial growth (Table 6; Figure 24).

| | | Pearson correlation | | | | | | | |
|---|---|---|---|---|---|---|---|---|---|
| | | A | M | J | J | A | S | apr-set | year |
| Tmax | D | -0.08 | -0.16 | -0.08 | -0.15 | -0.05 | 0.06 | -0.14 | 0.00 |
| | ND | -0.04 | -0.18 | -0.10 | -0.05 | 0.04 | 0.09 | -0.07 | 0.05 |
| PREC | D | -0.02 | 0.39 | 0.18 | -0.09 | -0.05 | -0.18 | 0.10 | 0.18 |
| | ND | -0.06 | 0.39 | 0.18 | -0.05 | -0.11 | -0.11 | 0.11 | 0.17 |
| SPEI-3 | D | 0.29 | 0.33 | 0.31 | 0.38 | 0.12 | -0.04 | 0.35 | 0.27 |
| | ND | 0.22 | 0.33 | 0.27 | 0.31 | 0.05 | -0.09 | 0.27 | 0.26 |

**Table 6:** *Climate-Kh Pearson correlation matrix. The data used are the detrended anatomical series of D and ND trees. The values highlighted are significant.*

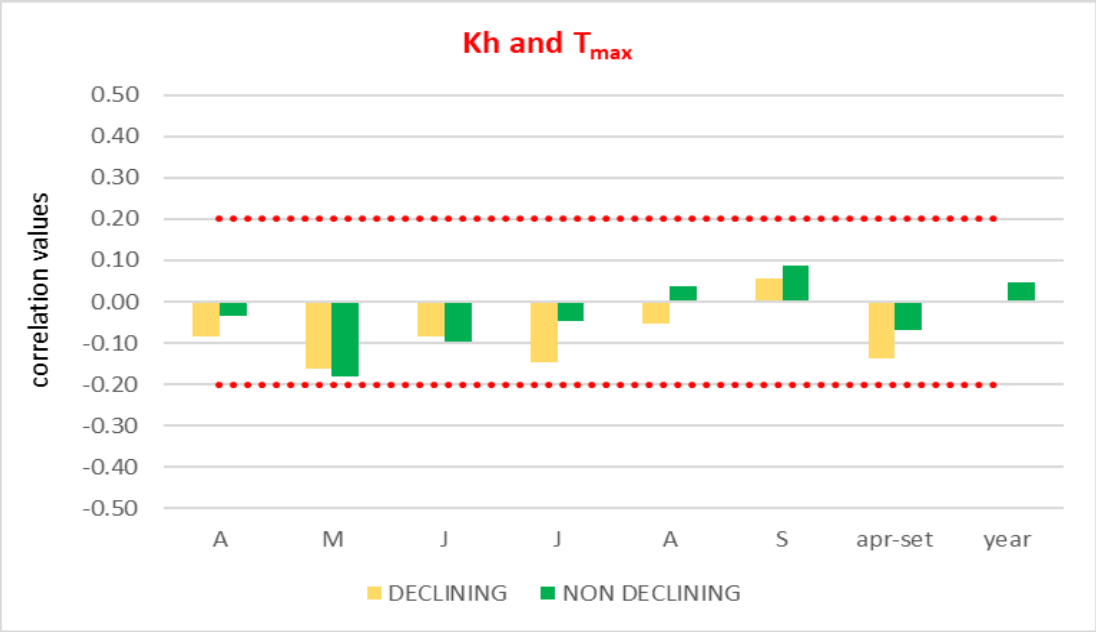


**Figure 24:** *Correlation between Tmax and detrended Kh (theoretical hydraulic conductivity) for declining (D) and non-declining (ND) series. The dashed red lines are the 0.05 significance thresholds.*

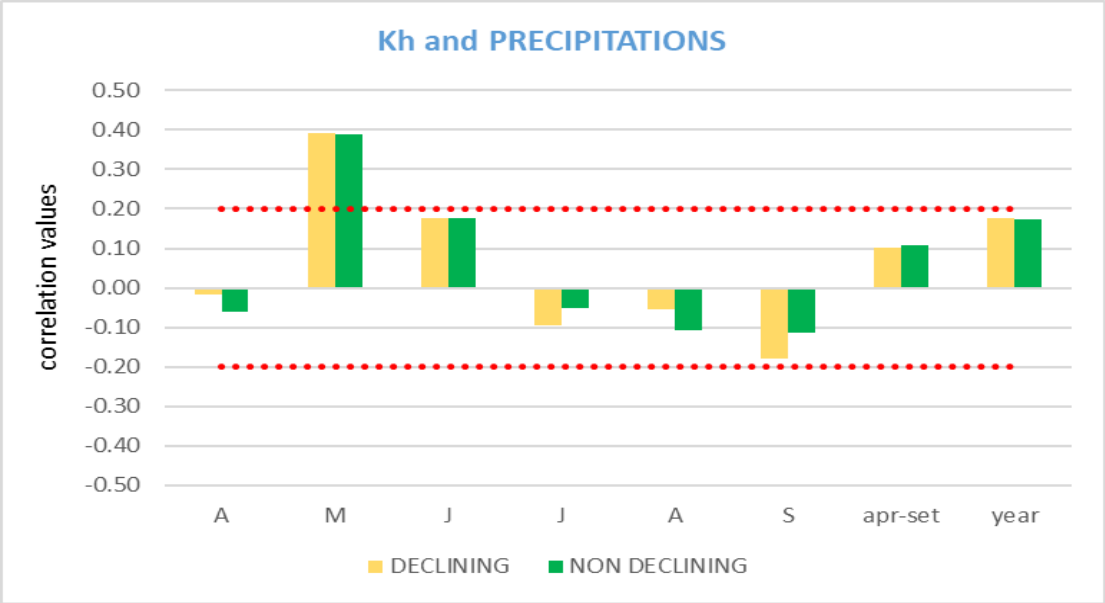


**Figure 25:** *Correlation between precipitations and detrended Kh (theoretical hydraulic conductivity) for declining (D) and non-declining (ND) series. The dashed red lines are the 0.05 significance thresholds.*

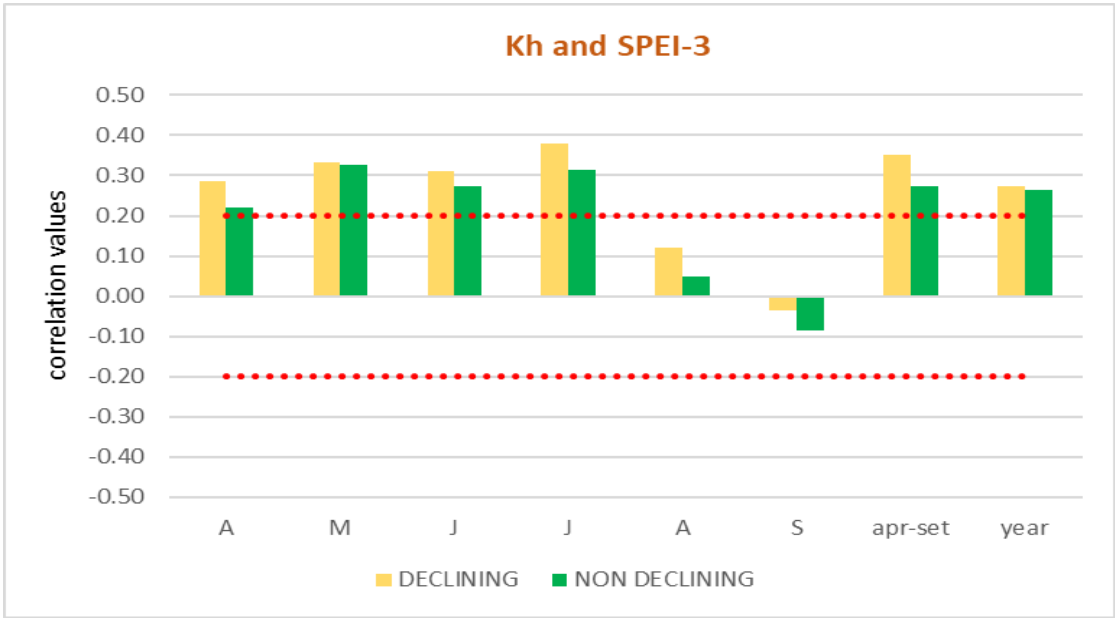


**Figure 26:** *Correlation between SPEI-3 and detrended Kh (theoretical hydraulic conductivity) for declining (D) and non-declining (ND) series. The dashed red lines are the 0.05 significance thresholds.*

### e) CWTtan: tangent cell wall thickness

CWTtan resulted significantly correlated to temperatures, precipitations and SPEI-3 during summer (**Table 7**; **Figure 27**; **Figure 28; Figure 29**) just for *declining* series, while there aren't correlations for *non-declining* series.

| | | Pearson correlation | | | | | | | |
|---|---|---|---|---|---|---|---|---|---|
| | | A | M | J | J | A | S | apr-set | year |
| Tmax | D | -0.06 | 0.06 | -0.13 | -0.26 | 0.11 | 0.11 | -0.04 | 0.02 |
| | ND | -0.17 | 0.06 | 0.00 | -0.10 | 0.17 | 0.09 | 0.01 | 0.02 |
| PREC | D | -0.02 | -0.04 | 0.38 | 0.15 | 0.08 | -0.04 | 0.20 | 0.24 |
| | ND | 0.03 | -0.04 | 0.16 | 0.05 | 0.00 | 0.00 | 0.07 | 0.18 |
| SPEI-3 | D | 0.02 | 0.06 | 0.12 | 0.34 | 0.29 | 0.04 | 0.22 | 0.18 |
| | ND | 0.07 | 0.04 | 0.02 | 0.06 | 0.03 | -0.08 | 0.03 | 0.12 |

**Table 7:** *Climate-CWTtan Pearson correlation matrix. The data used are the detrended anatomical series of D and ND trees. The values highlighted are significant.*

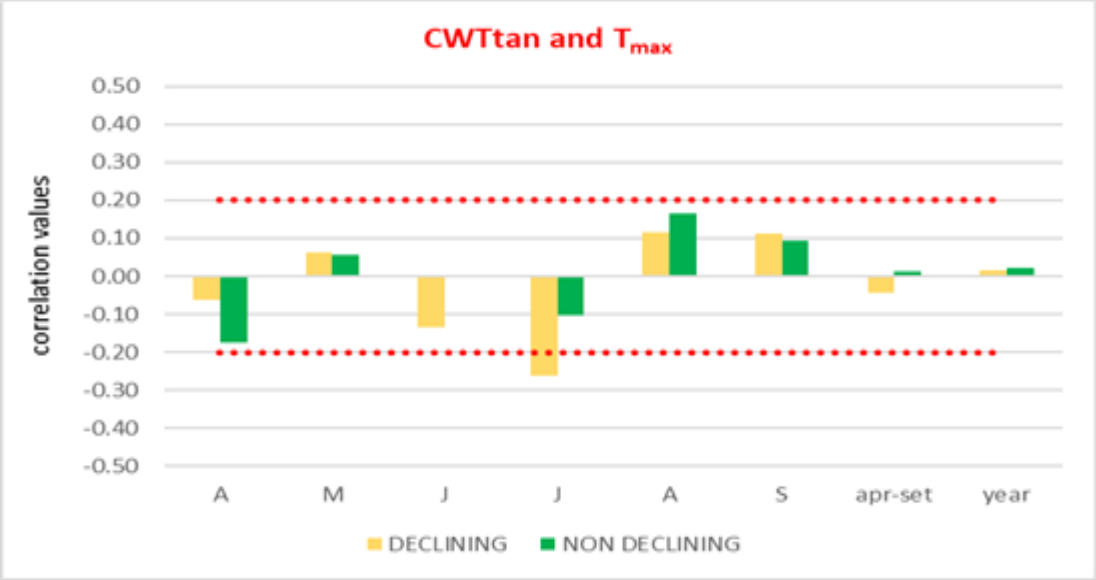


**Figure 27:** *Correlation between Tmax and detrended CWTtan (tangential cell wall thickness) for declining (D) and non-declining (ND) series. The dashed red lines are the 0.05 significance thresholds.*

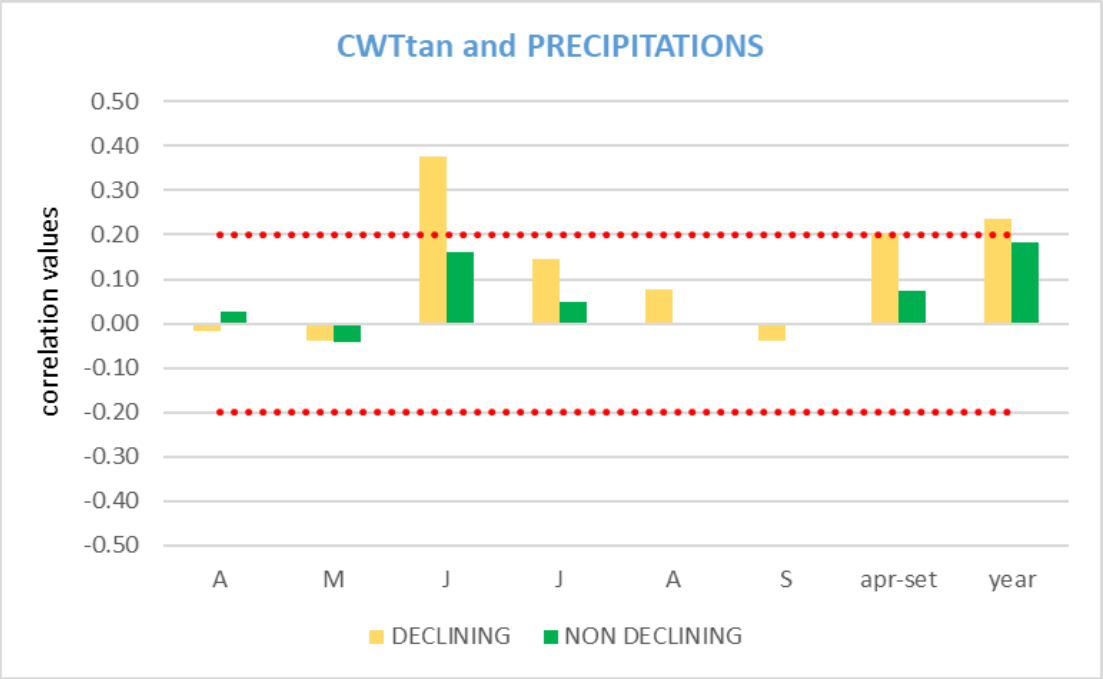


**Figure 28:** *Correlation between precipitations and detrended CWTtan (tangential cell wall thickness) for declining (D) and non-declining (ND) series. The dashed red lines are the 0.05 significance thresholds.*

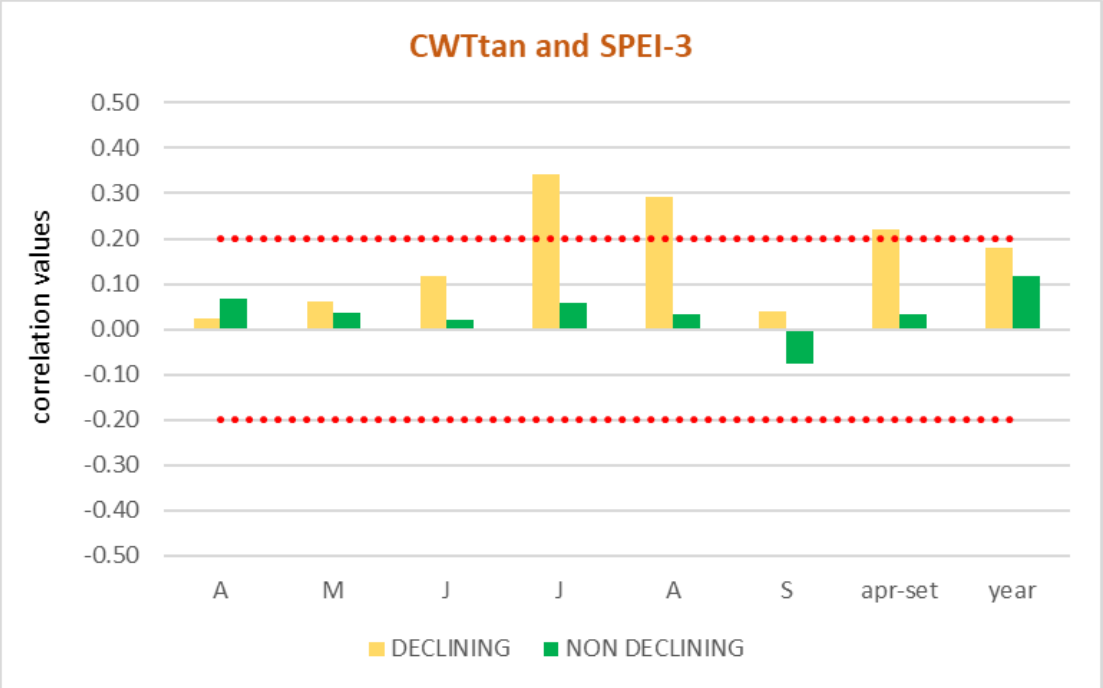


**Figure 29:** *Correlation between SPEI-3 and detrended CWTtan (tangential cell wall thickness) for declining (D) and non-declining (ND) series. The dashed red lines are the 0.05 significance thresholds.*

### f) LA 50%: cell lumen area at 50% percentile

LA50% resulted significantly correlated to temperatures, precipitations and SPEI-3 during spring and summer (Table 8; Figure 30; Figure 31; Figure 32).

| | | Pearson correlation | | | | | | | |
|---|---|---|---|---|---|---|---|---|---|
| | | A | M | J | J | A | S | apr-set | year |
| Tmax | D | 0.04 | -0.26 | -0.15 | 0.19 | -0.06 | -0.06 | -0.09 | -0.01 |
| | ND | 0.04 | -0.21 | -0.17 | 0.13 | -0.02 | -0.08 | -0.09 | -0.05 |
| PREC | D | 0.05 | 0.46 | -0.21 | -0.31 | -0.20 | -0.02 | -0.06 | -0.07 |
| | ND | 0.04 | 0.41 | 0.03 | -0.21 | -0.21 | -0.06 | 0.01 | -0.02 |
| SPEI-3 | D | 0.26 | 0.35 | 0.31 | 0.00 | -0.29 | -0.18 | 0.11 | 0.08 |
| | ND | 0.23 | 0.34 | 0.36 | 0.16 | -0.12 | -0.14 | 0.21 | 0.17 |

**Table 8:** *Climate-LA50% Pearson correlation matrix. The data used are the detrended anatomical series of D and ND trees. The values highlighted are significant.*

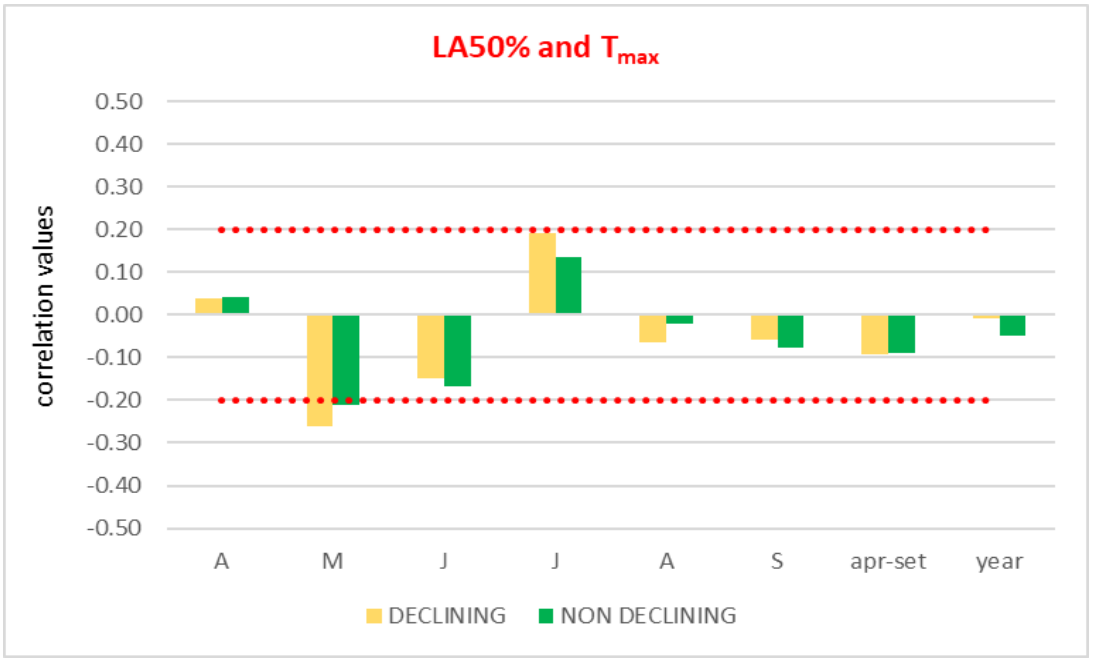


**Figure 30:** *Correlation between Tmax and detrended LA50% (cell lumen area at 50° percentile) for declining (D) and non-declining (ND) series. The dashed red lines are the 0.05 significance thresholds.*

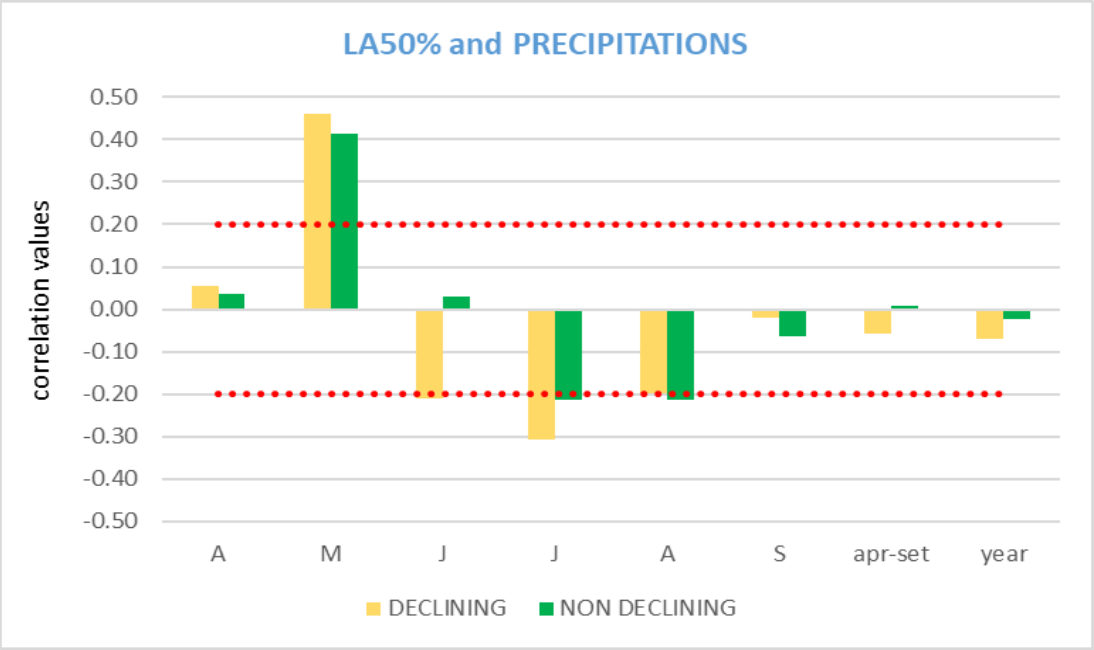


**Figure 31:** *Correlation between precipitations and detrended LA50% (cell lumen area at 50° percentile) for declining (D) and non-declining (ND) series. The dashed red lines are the 0.05 significance thresholds.*

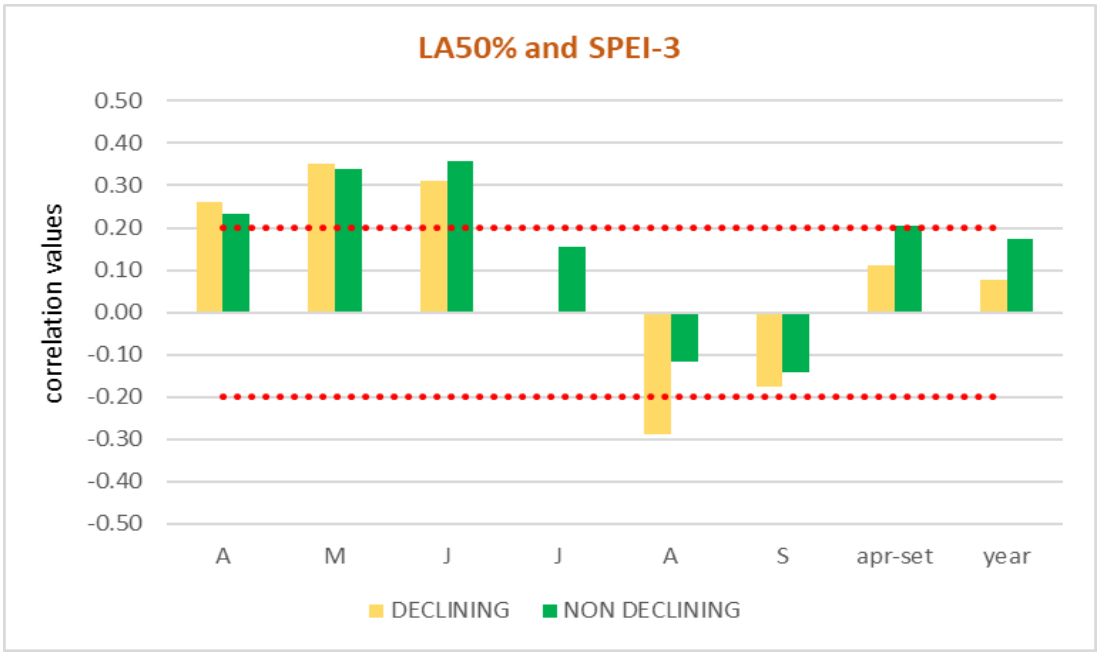


**Figure 32:** *Correlation between SPEI-3 and detrended LA50% (cell lumen area at 50° percentile) for declining (D) and non-declining (ND) series. The dashed red lines are the 0.05 significance thresholds.*

# 4) DISCUSSION

The climate associations with growth and xylem anatomical parameters analysed in the present work permit to observe and investigate the Austrian pine sensitivity to the climatic variables growing in an inner dry valley in the Alps.
To facilitate the discussion flow, the observations will be divided according to the climatic variable under analysis: annual average maximum temperature, annual precipitations and average SPEI-3.

- **Maximum temperature ($T_{max}$):** this variable shows rather poor correlations with MRW and Kh. On the other hand, negative correlations with Dh, CWTtan and LA50% are more significant in *declining* trees than *non-declining*, for which, the only (positive) correlation is with CNo.
- **Precipitations:** this variable has much stronger correlations with xylem parameters than temperatures. Both *declining* and *non-declining* trees show positive correlations for MRW, CNo, Dh, Kh and LA50%: an increase in summer rainfalls leads to an increase in the values of these parameters.
- **SPEI-3:** among the climatic variables, this is the one with the strongest associations with xylem parameters. Also in this case, the *declining trees* are more sensitive. However, it must be considered that an increase in SPEI-3 represents a wetter and not drier climate. It follows that, this variable establishes positive correlations with MRW, CNo, Dh, Kh, CWTtan and LA50%.

From these results, it emerges that *declining* trees tend to present a higher sensitivity to climate than *non-declining* ones. However, the differences between the time series of xylem traits of two groups (*D-ND*) are rather small and hardly significant apart a few single pointer years as e.g., 1996 or 2007.
This could mean that, unlike what found in the literature (Pellizzari et al., 2016; Puchi et al., 2020), *declining* Austrian pines in Venosta valley did not feature a progressive decline, but rather an abrupt die-off likely induced by sudden and unprecedented disturbance event that was decisive to determine the death of some trees.

Nonetheless, further considerations can be made by observing the detrended anatomical series, (especially MRW and Kh) in the last decades, where the 1996 and 2007 appears as decisive years in the differentiation of the *D* and *ND* groups (other detrended series are available on **ANNEX 2**). Looking at the climatic data referring to those years, it is possible to observe that both (1996 and 2007) are not the driest years of the reference time period (1942-2016). For example, 1996 was a moderately rainy year with an annual mean SPEI-3 value of 0.41 thus categorizing it as a slightly humid year. On the other hand, 2007 was clearly drier, with higher annual mean temperature and lower precipitations rate than 1996 (**Figure 33**).

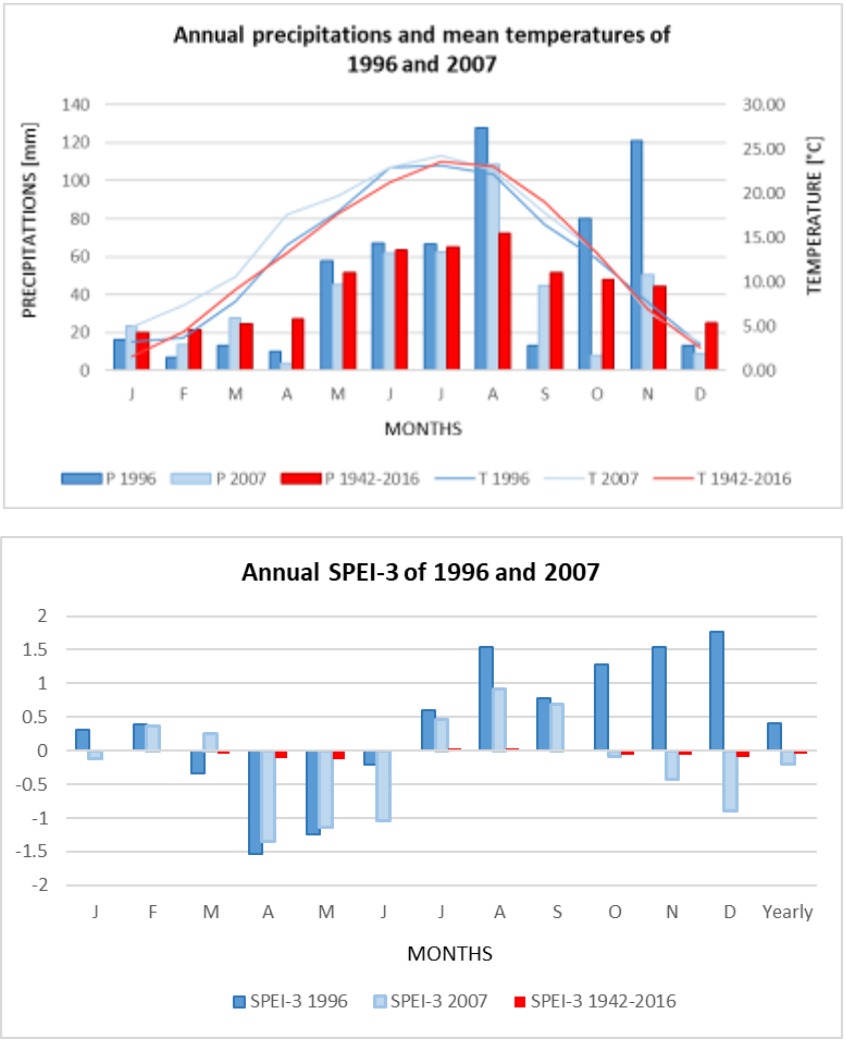


**Figure 33:** *Above: annual precipitations and annual mean temperatures of 1996, 2007 and the period 1942-2016; Below: annual SPEI-3 drought index and annual mean values of 1996, 2007 and the period 1942-2016. The data refer to the coordinates of the study site and were provided by CNR-ISAC (Bologna, IT; Brunetti et al., 2004, 2006).*

However, despite the slight drought, 2007 cannot be considered the hardest year for *Pinus nigra* in Venosta valley. Consequently, the significant divergence in those years, between *declining* and *non-declining* trees, could be caused by other external abiotic or biotic factors such as a single frost event or (more likely) a pest outbreaks, who may have taken advantage of the weaknesses of some trees (Klemm, 2019; Manion, 1991).

This major vulnerability to pests, especially for *declining* Austrian pines, could be related by the constrained cellular metabolism due to low water potentials which limited production and translocation of resin, crucial against insect attacks (Allen et al., 2010). Generally, *Pinus nigra*, as stated by Forner et al. (2014) *"maintains an isohydric performance under water stress conditions, which means tight control of stomata closure. However, under extreme drought this strategy could result in carbon starvation"* and a consequent general weakness.

However, for the tree responses it is also important to stress not just the role of the current year and current climate, but also what happened the year before. Indeed, as previously observed in several species, the presence of carry-over effects is sometimes as, or even more important, respect the immediate species responses (Babst et al. 2012).

Going back in time and looking at the precipitations, temperature and SPEI-3 data from 2002, it can be seen how that year was one of the wettest of the entire climatic record. These climatic characteristics are reflected on the xylem anatomical traits as MRW and Kh, where it is possible to see a separation of *declining* and *non-declining* trees, with the former having higher values. The following year (2003), was the opposite respect 2002, with very low precipitation, extremely high temperature and with a very low SPEI-3 index, especially during growing season, during which almost reached a value of -2 (**Figure 9**, chapter 2.1), therefore severely dry. The effects of this severe drought in 2003, counterintuitively, did not reduced tree growth rates (Allen et al., 2010) and post-drought resilience capacity (Bigler et al., 2007), as it was observed in many other species. In fact, we can note when looking at the anatomical series that during this climatic and ecological harsh year, Austrian pines, both *D* and *ND*, did not show a significant change in the value of the parameters, which instead took place, in a drastic and dramatic way, the following years. This

confirms what Forner et al., (2014) stated, that Austrian pine is subjected to one-year delay in growth response to drought based on previous climatic conditions.

These concomitances of climatic events, well reflected in the trees anatomical parameters, could be justified by the lag effects of drought and the role of compound disturbances, which may result in a lagged forest decline (Bigler et al., 2007), and predispose *declining* trees more easily to insect outbreaks (as it happened in 2007) and finally, leading to have such a wide distinction in the values of the anatomical parameters between *D* and *ND* Austrian pines.

Finally, it is important to underline again how the sudden mortality of certain trees, should be due to some other factors such as one punctual and decisive episode or more subsequent extreme events and/or a pest outbreak, rather than the long-lasting drought of the study area.

# 5) CONCLUSIONS

In a context of current climate change and increasingly frequent and prolonged droughts, it is necessary to have an accurate understanding of the forest response to this variability.

The prediction of the future responses of certain forest species and understanding which intra-specific anatomical characteristics can lead to forest decline, could be useful for several purposes. Future forest management, forecasting models to identify the future geographic distribution of tree species, the identification of forest communities' vitality and, lastly, the choice of indicators for past drought events (useful for climatic reconstruction) could benefit from the contribution of these kind of predictions.

Wood anatomical traits, in combination with long-term climate records can be successfully used as proxy data, providing excellent information about past droughts events and about how forests could react in the future.

In this thesis, the analysis of the anatomical xylem parameters and their associations with climatic data, made it possible to find what are the climatic sensitivity of *Pinus nigra* in Venosta valley (Italian Alps).

In contrast to our initial hypothesis, we didn't show substantial differences between the two groups of *declining* and *non-declining* trees: thus, in this case, we did not identify any anatomical and physiological differences to directly associate to the mortality event, however it's still important to underline the complexity of environmental interactions and compound effects which play a significant role in the mortality in some forest stands.

This thesis therefore, underlines how intricate and necessary is to deepen the climate-anatomical traits correlations, especially in those forest stands where the decline is already ongoing. It therefore encourages research on this topic, leaving room for further study.

## 6) BIBLIOGRAPHY


Aimi, A., Zocca, A., Minerbi, S., & Hellrigl, K., et al. (2006). The outbreak of the pine processionary moth in Venosta/Vinschgau: ecological and economic aspects. *Forest Observer, 2/3*, 69–80.

Allen, C. D., Macalady, A. K., Chenchouni, H., Bachelet, D., McDowell, N., Vennetier, M., … Cobb, N. (2010). A global overview of drought and heat-induced tree mortality reveals emerging climate change risks for forests. *Forest Ecology and Management*, *259*(4), 660–684. https://doi.org/10.1016/j.foreco.2009.09.001

Anderegg, W. R. L., Schwalm, C., Biondi, F., Camarero, J. J., Koch, G., Litvak, M., … Pacala, S. (2015). Pervasive drought legacies in forest ecosystems and their implications for carbon cycle models. *Science*, *349*(6247), 528–532. https://doi.org/10.1126/science.aab1833

Aniol, R. W. (1983). Tree-ring analysis using CATRAS. *Dendrochronologia*, *1*(1), 45-53.

Aniol, R. W. (1987). A new device for computer assisted measurement of tree-ring widths. *Dendrochronologia*, *5*, 135-141.

Autonome Provinz Bozen-Südtirol (Hg.) (2010). *Waldtypisierung Südtirol Band 2. Waldgruppen, Naturräume, Glossar*.

Babst, F., Carrer, M., Poulter, B., Urbinati, C., Neuwirth, B., & Frank, D. (2012). 500 years of regional forest growth variability and links to climatic extreme events in Europe. *Environmental Research Letters*, *7*(4), 045705.

Barber, V. A., Juday, G. P., Finney, B. P. (2000). Reduced growth of Alaskan white spruce in the twentieth century from temperature-induced drought stress, *405*(June).

Bigler, C., Gavin, D.G., Gunning, C., & Veblen, T.T. (2007). Drought induces lagged tree mortality in a subalpine forest in the Rocky Mountains. *Oikos, 116(12)*, 1983–1994. DOI 10.1111/j.2007.0030-1299.16034.x.

Blasing, T. J., & Fritts, H. C. (1976). Reconstructing past climatic anomalies in the North Pacific and western North America from tree-ring data. *Quaternary Research*, *6*(4), 563-579.

Brunetti, M., Buffoni, L., Mangianti, F., Maugeri, M., Nanni, T. (2004).

Temperature, precipitation and extreme events during the last century in Italy. *Global and Planetary Change*, *40*(1–2), 141–149. https://doi.org/10.1016/S0921-8181(03)00104-8

Brunetti, M., Maugeri, M., Nanni, T., Auer, I., Böhm, R., Schöner, W. (2006). Precipitation variability and changes in the greater Alpine region over the 1800–2003 period. *Journal of Geophysical Research: Atmospheres*, *111*(D11), 11107. https://doi.org/10.1029/2005JD006674

Buscarini, S., Tonon, G., Oberhuber, W., Obojes, N. (2019). *Comparison of climate-growth relations of different conifers along elevation gradients in an inner-alpine dry valley*. Università di Bolzano, Universitaat Innsbruck.

Carrer, M., Von Arx, G., Castagneri, D., Petit, G. (2015). Distilling allometric and environmental information from time series of conduit size: The standardization issue and its relationship to tree hydraulic architecture. *Tree Physiology*, *35*(1), 27–33. https://doi.org/10.1093/treephys/tpu108

Cook, E. R. (1990). A conceptual linear aggregate model for tree rings. *Methods of Dendrochronology: Applications in the Environmental Sciences*, *104*(3), 98–103.

Enescu, C. M., de Rigo, D., Caudullo, G., Mauri, A., Houston Durrant, T. (2016). Pinus nigra in Europe: distribution, habitat, usage and threats. *European Atlas of Forest Tree Species*, *Publ.Off.E*, e015138.

Forner, A., Aranda, I., Granier, A., & Valladares, F. (2014). *Differential Impact of the Most Extreme Drought Event Over the Last Half Century on Growth and Sap Flow in Two Coexisting Mediterranean Trees*. *Plant Ecology, 215(7)*, 703–719. DOI 10.1007/s11258-014-0351-x.

Girardin, M. P., Guo, X. J., De Jong, R., Kinnard, C., Bernier, P., Raulier, F. (2014). Unusual forest growth decline in boreal North America covaries with the retreat of Arctic sea ice. *Global Change Biology*, *20*(3), 851–866. https://doi.org/10.1111/gcb.12400

Grissino-Mayer, H. D. (2001). Evaluating crossdating accuracy: a manual and tutorial for the computer program COFECHA.

Hacke, U. (2001). Functional and ecological Xylem anatomy. *Functional and Ecological Xylem Anatomy*,*4*,1–281. https://doi.org/10.1007/978-3-319-15783-2

IPCC. (2021). *Summary for Policymakers. Contribution of Working Group I to the Sixth Assessment Report of the Intergovernmental Panel on Climate Change*. *Climate Change 2021: The Physical Science Basis.*

Jones, H. G. (1998). Stomatal control of photosynthesis and transpiration. *Journal of experimental botany*, 387-398.

Kim, T. W., Jehanzaib, M. (2020). Drought risk analysis, forecasting and assessment under climate change. *Water (Switzerland)*, *12*(7), 1–7. https://doi.org/10.3390/W12071862

Klemm, J. (2019). *Remote sensing and dendrochronological based quantification of vitality decline of Black pine stands in the Vinschgau region, Italy*. Julius Maximilian University of Würzburg.

Körner, C. (2003). Carbon limitation in trees. *Journal of Ecology*, *91*(1), 4–17. https://doi.org/10.1046/j.1365-2745.2003.00742.x

Lebourgeois, F., Rathgeber, C., & Ulrich, E. (2010). Sensitivity of French temperate coniferous forests to climate variability and extreme events (Abies alba, Picea abies and Pinus sylvestris). *Journal of Vegetation Science (21)*, 364–376.

Manion, P. d. (1991). *Tree Disease Concepts*. Englewood Cliffs, N.J.: Prentice-Hall.

Mariani, S., Braca, G., Romano, E., Lastoria, B., Bussettini, M. (2018). *Guidelines on indicators of drought and water scarcity to be used in the activities of permanent observators for water use current status and future perspectives*.

Martin-Benito, D., Anchukaitis, K. J., Evans, M. N., del Río, M., Beeckman, H., Cañellas, I. (2017). Effects of drought on xylem anatomy and water-use efficiency of two co-occurring pine species. *Forests*, *8*(9), 1–19. https://doi.org/10.3390/f8090332

Martínez-Vilalta, J.; Poyatos, R.; Aguadé, D.; Retana, J.; Mencuccini, M. (2014). A new look at water transport regulation in plants. New Phytol. 204, 105–115.

Mauro, G. (2017). Cambiamenti Climatici E Foreste Nell'Area Alpina: Telerilevamento a Bassa Risoluzione Spaziale Per Il Monitoraggio Della Vegetazione Boschiva, (April).

McDowell, N., Pockman, W. T., Allen, C. D., Breshears, D. D., Cobb, N., Kolb, T., … Yepez, E. A. (2008). Mechanisms of plant survival and mortality during drought: Why do some plants survive while others succumb to drought? *New*

*Phytologist*, *178*(4), 719–739. https://doi.org/10.1111/j.1469-8137.2008.02436.x

McElrone, A. J., Choat, B., Gambetta, G. A., & Brodersen, C. R. (2013). Water uptake and transport in vascular plants. *Nature Education Knowledge*, *4*(5), 6.

Mukherjee, S., Mishra, A., Trenberth, K. E. (2018). Climate Change and Drought: a Perspective on Drought Indices. *Current Climate Change Reports*, *4*(2), 145–163. https://doi.org/10.1007/s40641-018-0098-x

Nardini, A., Battistuzzo, M., & Savi, T. (2013). Shoot desiccation and hydraulic failure in temperate woody angiosperms during an extreme summer drought. *New Phytologist*, *200*(2), 322-329.

Pan, Y., Birdsey, R. A., Fang, J., Houghton, R., Kauppi, P. E., Kurz, W. A., … Hayes, D. (2011). A large and persistent carbon sink in the world's forests. *Science*, *333*(6045), 988–993. https://doi.org/10.1126/science.1201609

Pellizzari, E., Camarero, J. J., Gazol, A., Sangüesa-Barreda, G., Carrer, M. (2016). Wood anatomy and carbon-isotope discrimination support long-term hydraulic deterioration as a major cause of drought-induced dieback. *Global Change Biology*, *22*(6), 2125–2137. https://doi.org/10.1111/gcb.13227

Puchi, P. F., Castagneri, D., Rossi, S., Carrer, M. (2020). Wood anatomical traits in black spruce reveal latent water constraints on the boreal forest. *Global Change Biology*, *26*(3), 1767–1777. https://doi.org/10.1111/gcb.14906

Rossi, S., Deslauriers, A., & Anfodillo, T. (2006). Assessment of cambial activity and xylogenesis by microsampling tree species: an example at the Alpine timberline. *Iawa Journal*, *27*(4), 383-394.

Sala, A., Piper, F., Hoch, G. (2010). Physiological mechanisms of drought-induced tree mortality are far from being resolved. *New Phytologist*, 264–266.

Savi, T., Casolo, V., Dal Borgo, A., Rosner, S., Torboli, V., Stenni, B., Nardini, A. (2019). Drought-induced dieback of Pinus nigra: A tale of hydraulic failure and carbon starvation. *Conservation Physiology*, *7*(1), 1–12. https://doi.org/10.1093/conphys/coz012

Speer, J. H. (2010). *Fundamentals of tree-ring research*. University of Arizona Press.

Team, R. C. (2013). R: A language and environment for statistical computing.

Tyree, M. T., & Ewers, F. W. (1991). The hydraulic architecture of trees and other

woody plants. *New Phytologist*, *119*(3), 345-360.

Vicente-Serrano, S. M., Beguería, S., & López-Moreno, J. I. (2010). A multiscalar drought index sensitive to global warming: the standardized precipitation evapotranspiration index. *Journal of climate*, *23*(7), 1696-1718.

Von Arx, G., & Carrer, M. (2014). ROXAS–A new tool to build centuries-long tracheid-lumen chronologies in conifers. *Dendrochronologia*, *32*(3), 290-293.

Walker, X., Johnstone, J. F. (2014). Widespread negative correlations between black spruce growth and temperature across topographic moisture gradients in the boreal forest. *Environmental Research Letters*, *9*(6). https://doi.org/10.1088/1748-9326/9/6/064016

## 7) SITOGRAPHY

- Autorità di bacino nazionale del fiume Adige, (2022). Extrapolated from http://www.bacinoadige.it/info_bacino/index.php?i=82&p=sottobacini#:~:text=L'Adige%20fino%20a%20Bolzano,colture%20di%20verdura%20o%20malghe on 19 January 2022.

- N.p., "Flora e fauna della Val Venosta in Alto Adige. Tutta la diversità delle Alpi in una valle". *Venosta.net,* (n.d.). Extrapolated from https://www.venosta.net/it/cultura-arte/paesaggio-naturale/flora-fauna.html on 18 December 2021.

## 8) INDEX OF FIGURES

# 9) INDEX OF TABLES

## **ANNEX 1:** raw anatomical series aligned with years and with age

YEARS TRENDS with logarithmic scale.

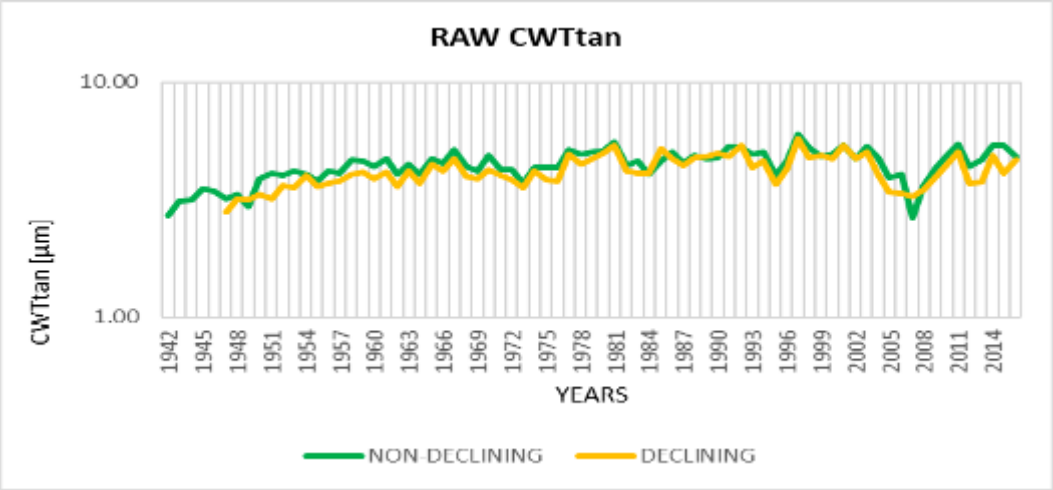


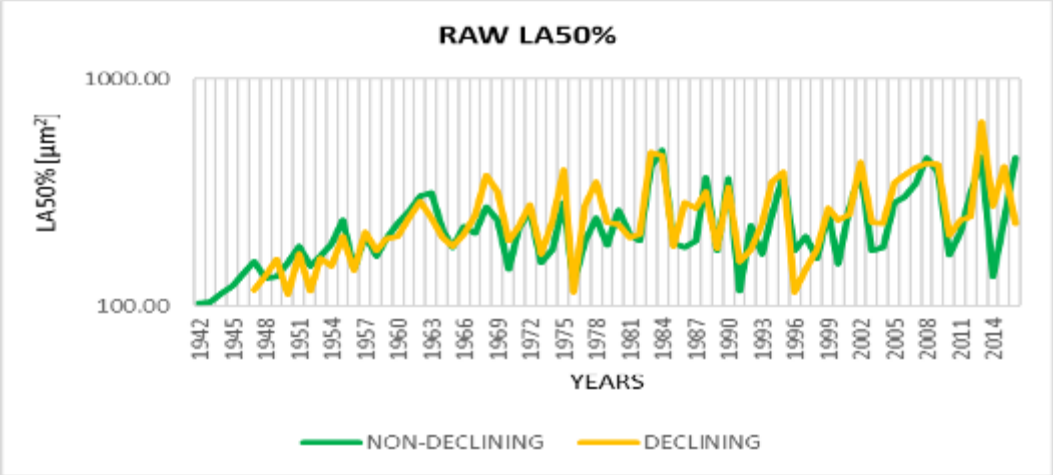


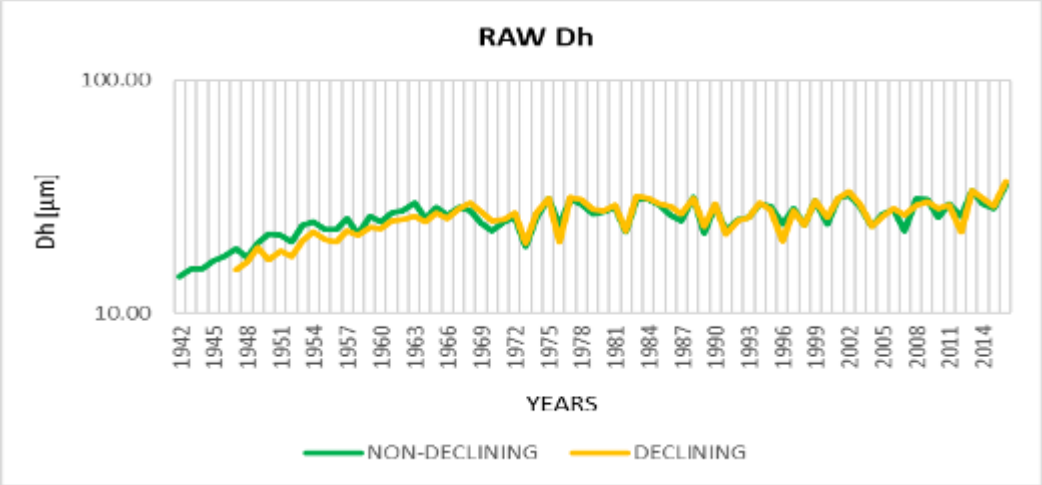

AGE TRENDS with logarithmic scale.

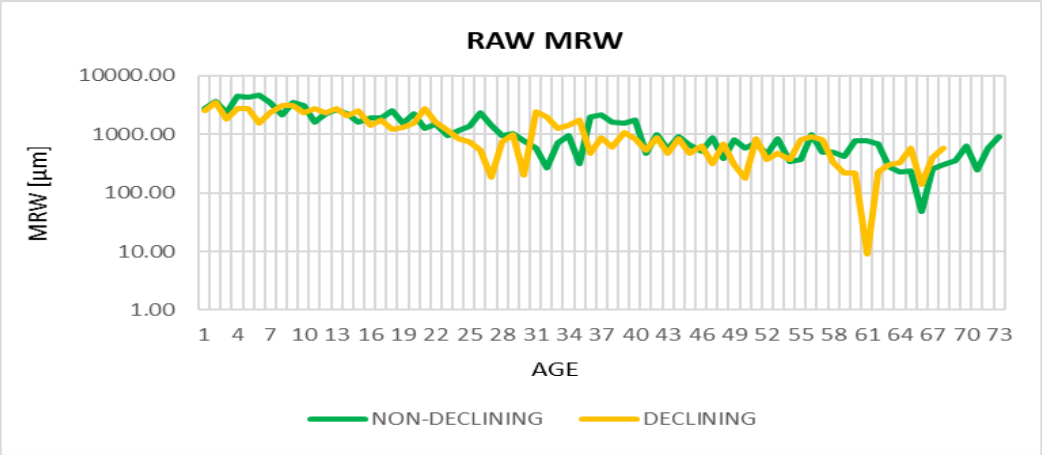


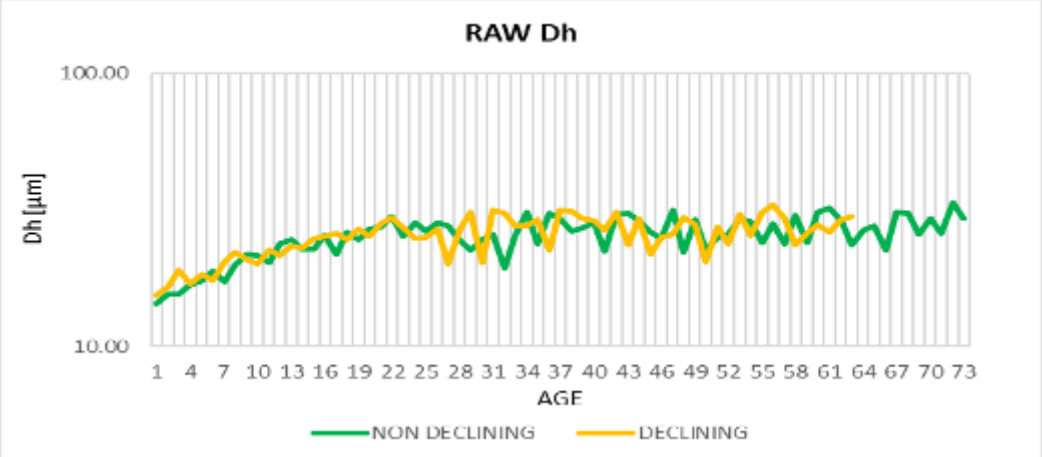


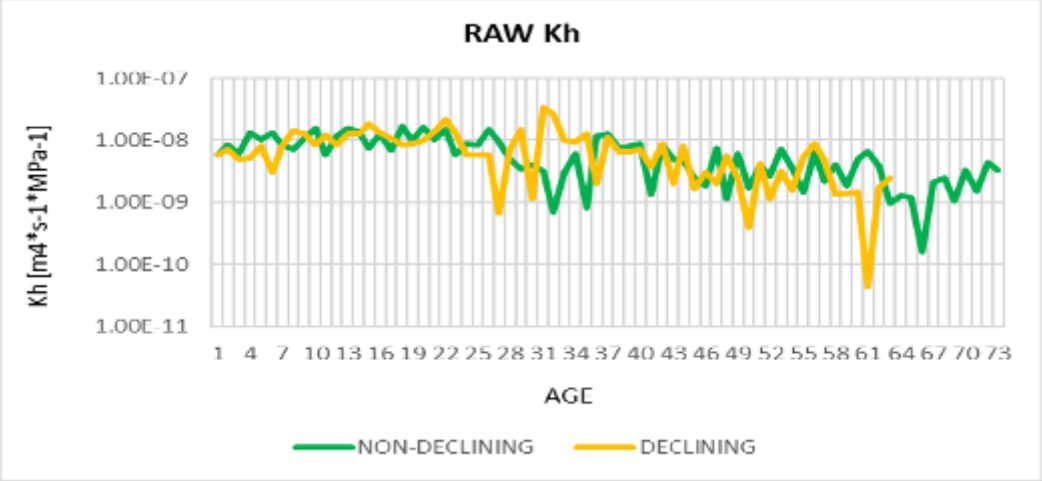

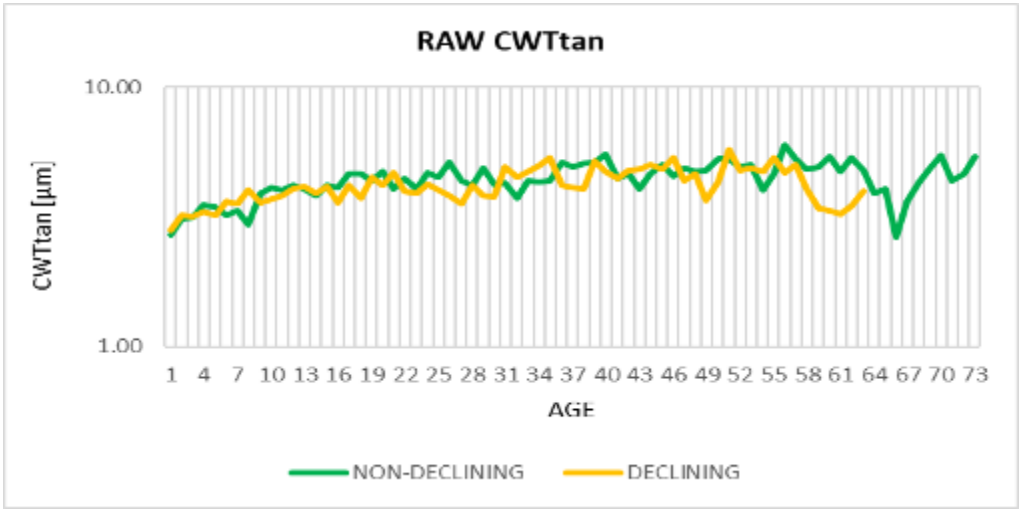
RAW CWTtan
10.00
1.00
CWTtan [µm]
1 4 7 10 13 16 19 22 25 28 31 34 37 40 43 46 49 52 55 58 61 64 67 70 73
AGE
NON-DECLINING
DECLINING

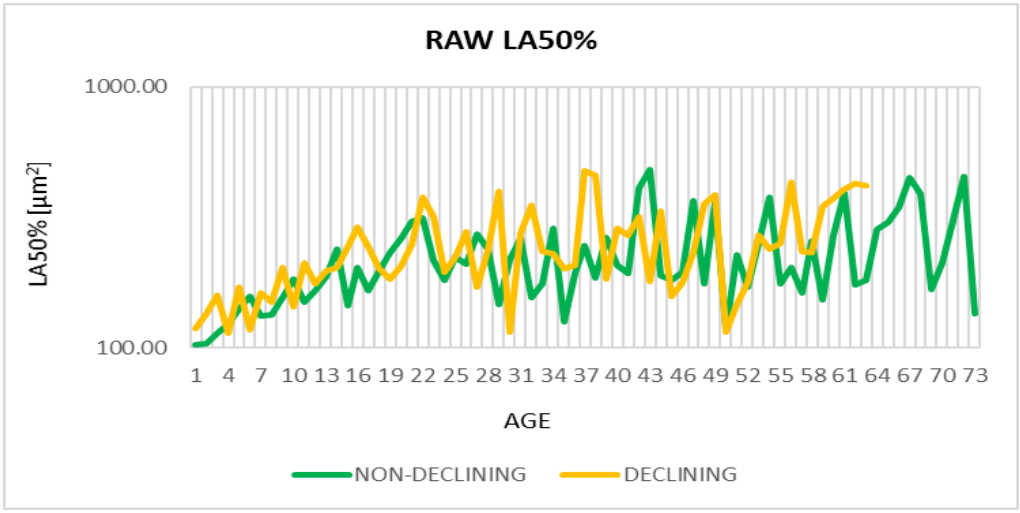
RAW LA50%
1000.00
100.00
LA50% [µm²]
1 4 7 10 13 16 19 22 25 28 31 34 37 40 43 46 49 52 55 58 61 64 67 70 73
AGE
NON-DECLINING
DECLINING

## **ANNEX 2**: detrended anatomical series aligned with years and age

YEARS TRENDS with logarithmic scale.

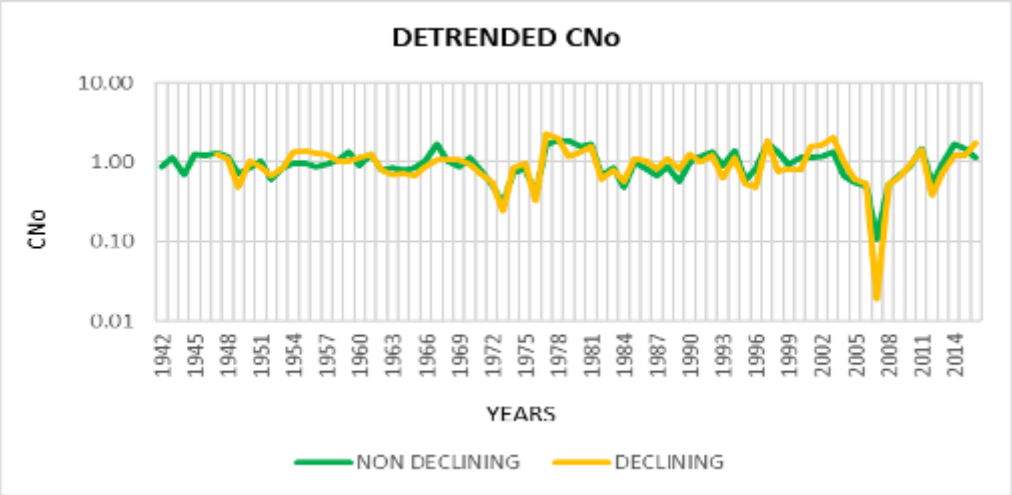


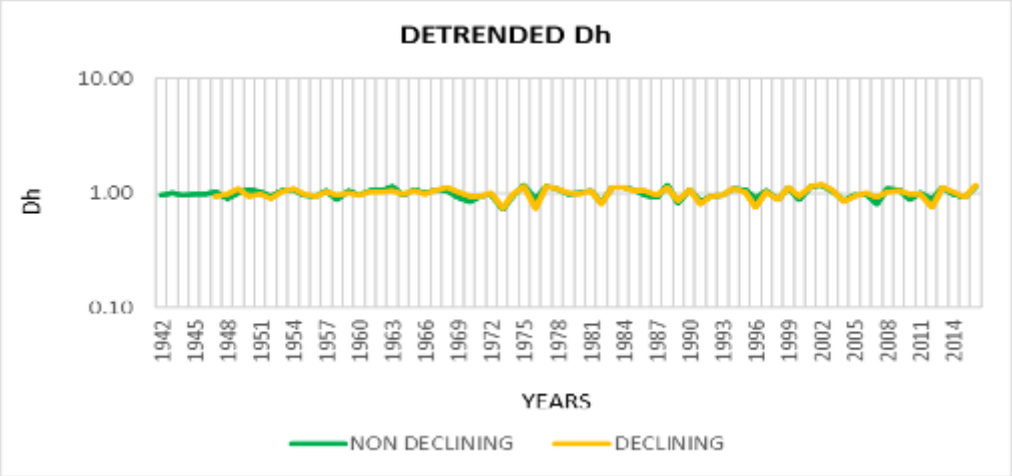


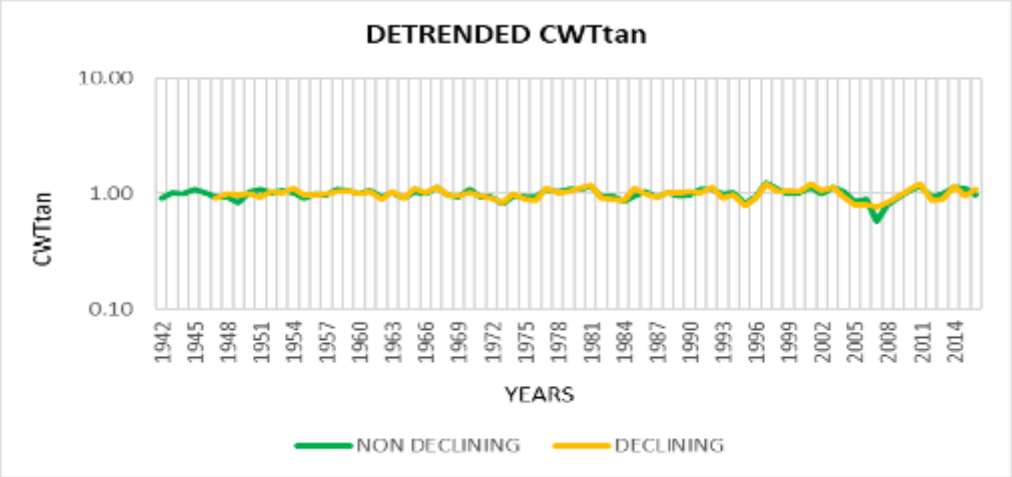

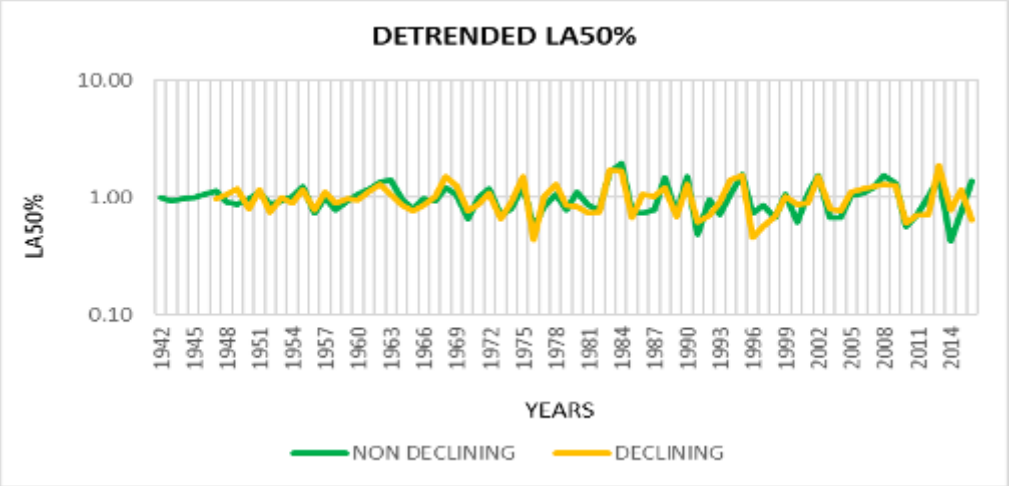


AGE TRENDS with logarithmic scale.

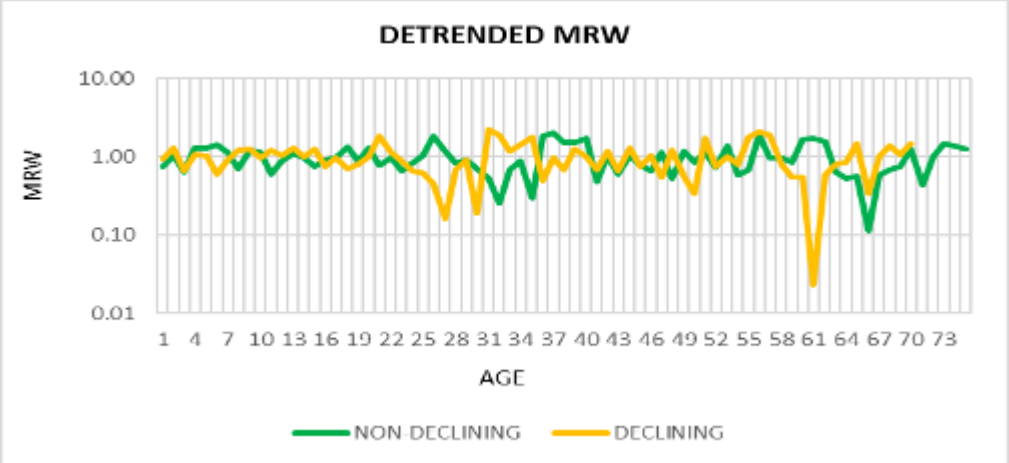


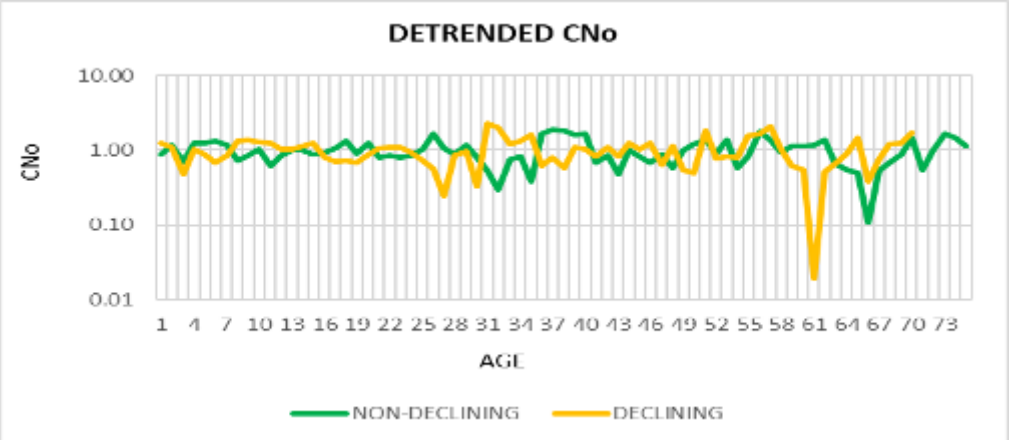

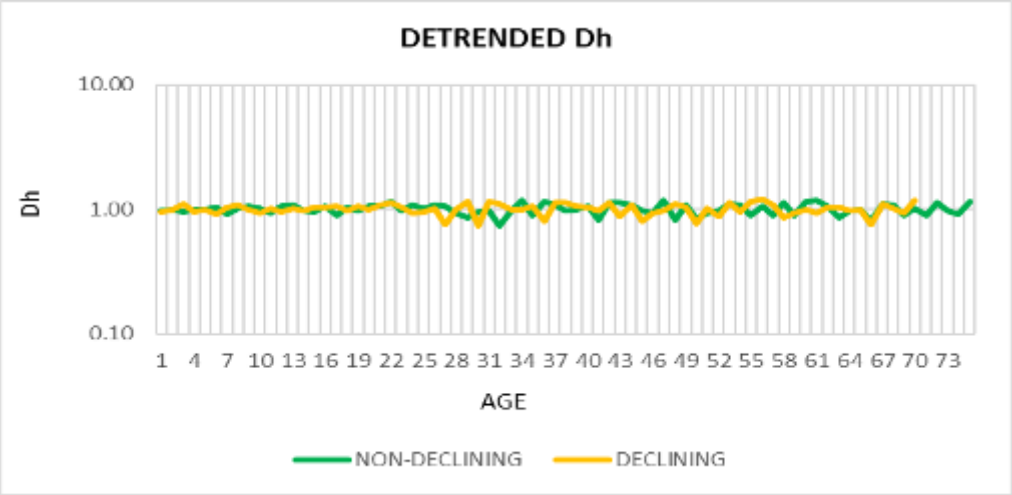
DETRENDED Dh
10.00
1.00
0.10
Dh
1 4 7 10 13 16 19 22 25 28 31 34 37 40 43 46 49 52 55 58 61 64 67 70 73
AGE
NON-DECLINING
DECLINING

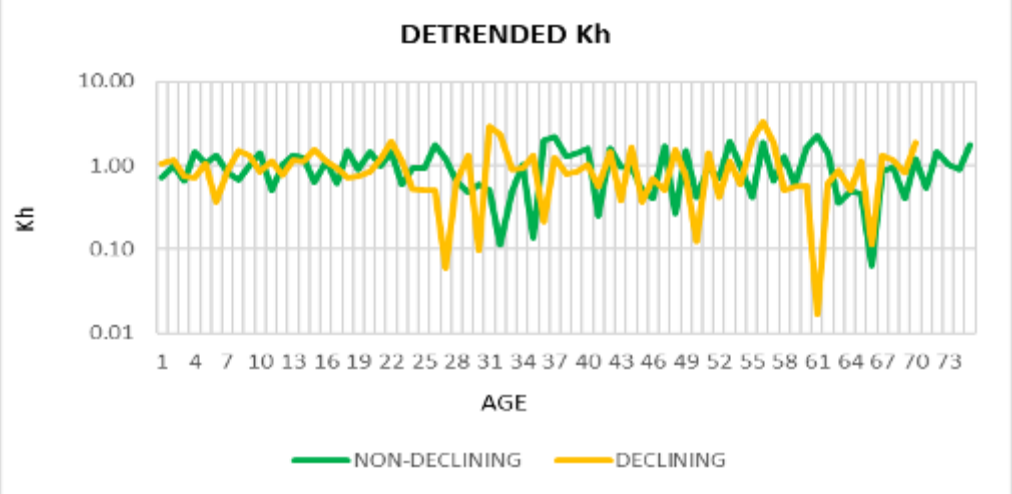
DETRENDED Kh
10.00
1.00
0.10
0.01
Kh
1 4 7 10 13 16 19 22 25 28 31 34 37 40 43 46 49 52 55 58 61 64 67 70 73
AGE
NON-DECLINING
DECLINING

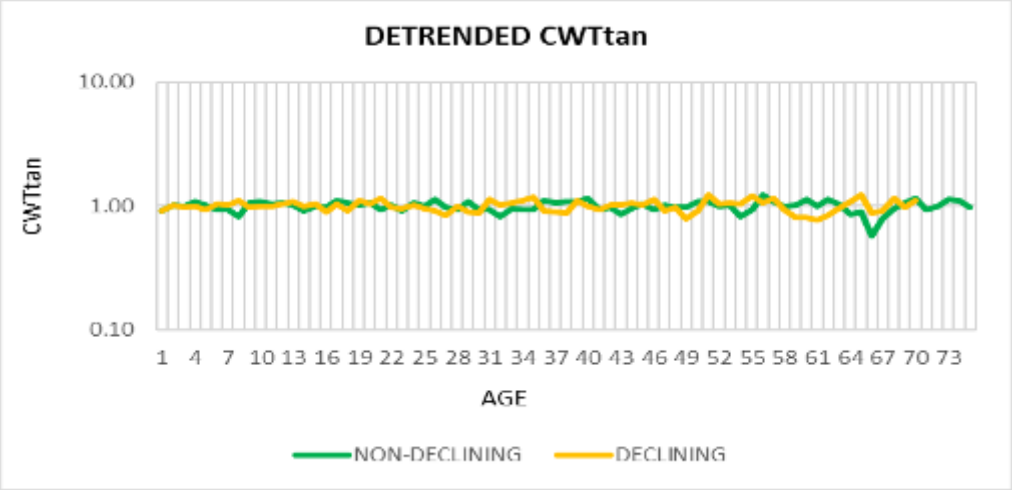
DETRENDED CWTtan
10.00
1.00
0.10
CWTtan
1 4 7 10 13 16 19 22 25 28 31 34 37 40 43 46 49 52 55 58 61 64 67 70 73
AGE
NON-DECLINING
DECLINING

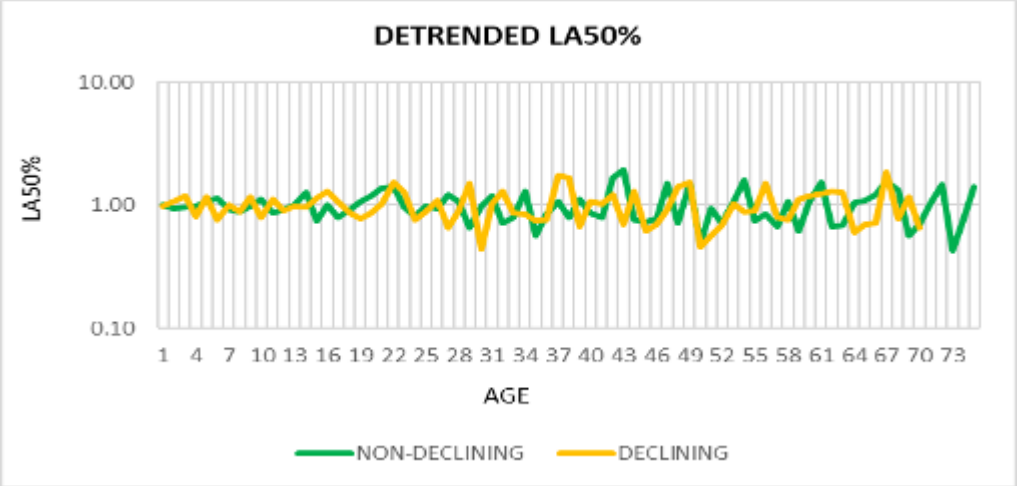
DETRENDED LA50%
10.00
1.00
0.10
LA50%
1 4 7 10 13 16 19 22 25 28 31 34 37 40 43 46 49 52 55 58 61 64 67 70 73
AGE
NON-DECLINING
DECLINING